The International Journal of Robotics Research

http://ijr.sagepub.com/

Published by:
$SAGE

http://www.sagepublications.com

On behalf of:

ijrr

Multimedia Archives

Additional services and information for *The International Journal of Robotics Research* can be found at:

Email Alerts: http://ijr.sagepub.com/cgi/alerts

Subscriptions: http://ijr.sagepub.com/subscriptions

Reprints: http://www.sagepub.com/journalsReprints.nav

Permissions: http://www.sagepub.com/journalsPermissions.nav

Citations: http://ijr.sagepub.com/content/29/12/1475.refs.html

Planning and Implementing Trajectories for Autonomous Underwater Vehicles to Track Evolving Ocean Processes Based on Predictions from a Regional Ocean Model

Ryan N. Smith[1], Yi Chao[2], Peggy P. Li[2], David A. Caron[3], Burton H. Jones[3] and Gaurav S. Sukhatme[1]

Abstract

Path planning and trajectory design for autonomous underwater vehicles (AUVs) is of great importance to the oceanographic research community because automated data collection is becoming more prevalent. Intelligent planning is required to maneuver a vehicle to high-valued locations to perform data collection. In this paper, we present algorithms that determine paths for AUVs to track evolving features of interest in the ocean by considering the output of predictive ocean models. While traversing the computed path, the vehicle provides near-real-time, in situ *measurements back to the model, with the intent to increase the skill of future predictions in the local region. The results presented here extend preliminary developments of the path planning portion of an end-to-end autonomous prediction and tasking system for aquatic, mobile sensor networks. This extension is the incorporation of multiple vehicles to track the centroid and the boundary of the extent of a feature of interest. Similar algorithms to those presented here are under development to consider additional locations for multiple types of features. The primary focus here is on algorithm development utilizing model predictions to assist in solving the motion planning problem of steering an AUV to high-valued locations, with respect to the data desired. We discuss the design technique to generate the paths, present simulation results and provide experimental data from field deployments for tracking dynamic features by use of an AUV in the Southern California coastal ocean.*

Keywords

1. Introduction

Coastal ocean regions are dynamic and complex environments that are driven by an intricate interaction between atmospheric, oceanographic, estuarine/riverine and land–sea processes. Effective observation and quantification of these processes requires the simultaneous measurement of diverse water properties to capture the spatial and temporal variability. The implementation of multiple and adaptable sensors can facilitate simultaneous and rapid measurements that capture the appropriate scale of spatiotemporal variability for many of the phenomena that we seek to understand occurring in the coastal ocean. Autonomous underwater vehicles (AUVs) are a key tool in this effective, efficient and adaptive data collection procedure to improve our overall understanding of coastal processes and our world's oceans. Through development of these intelligent systems, scientists can implement continuous monitoring and sampling programs that provide fine-scale resolution far surpassing previous sampling methods, such as infrequent measurements from ships, buoys and drifters. One

example of intelligent ocean sampling is the coordinated control of autonomous and Lagrangian platforms and sensors (ALPS), developed in the series of articles Fiorelli et al. (2006), Leonard et al. (2007), and Paley et al. (2007, 2008). Such research efforts have opened the door for the design and implementation of adaptive, mobile sensor platforms and networks to aid in the study of complex phenomena such as ocean currents, tidal mixing and other dynamic ocean processes.

[1] Robotic Embedded Systems Laboratory, University of Southern California, Los Angeles, CA 90089, USA
[2] Jet Propulsion Laboratory, California Institute of Technology, 4800 Oak Grove Drive, Pasadena, CA 91109, USA
[3] Department of Biological Sciences, University of Southern California, Los Angeles, CA 90089, USA

Corresponding author:
Ryan N Smith
Robotic Embedded Systems Laboratory
University of Southern California
Los Angeles, CA 90089
USA
Email: ryannsmi@usc.edu

To this end, three laboratories at the University of Southern California (USC) have formed CINAPS (pronounced [sin-aps]); the Center for Integrated Networked Aquatic Platforms. The mission of this collaborative research group is to bridge the gap between technology, communication and the scientific exploration of local and regional aquatic ecosystems through the implementation of an embedded sensor network along the Southern California coast (Smith et al. 2010a). This infrastructure is designed for facilitation of long-term, in-depth, multi-faceted investigation of physical, chemical and biological processes resulting from coastal urbanization and climate change. One component of this network, and the focus of this paper, are mobile sensor platforms in the form of autonomous Slocum gliders (gliders) (Webb Research Corporation 2008). Based on their deployment longevity, and the use of multiple gliders (see e.g. Davis et al. (2008)), these vehicles can provide an extended spatiotemporal series of observations (see details in Section 4). This study investigates a path planning method for a multi-vehicle application for gliders in the Southern California coastal ocean.

The path planning method presented here is based upon predictions from a regional ocean model. As complex and understudied as the ocean may be, we are able to model and predict certain behaviors moderately well over short time periods. Consistently comparing model predictions with collected data, and adjusting for discrepancies, will increase the range of validity of existing ocean models, both temporally and spatially.

Utilizing available technology and infrastructure, we consider the problem of integrating ocean model predictions into the path planning and trajectory design procedure for AUVs, with the goal of tracking and sampling within an interesting and evolving ocean feature. Collecting data for ocean science can be extremely hit-or-miss, both temporally and spatially, especially when one is interested in a specific biogeochemical event. In addition, areas of scientific interest within the ocean dynamically move and evolve. Thus, continuously operating a sensor platform (static or mobile) in a predesignated and confined sampling area is not the most effective technique to gather data for analysis and assessment of ocean processes which may occur sporadically, and dynamically propagate throughout the ocean. Here we aim to increase the likelihood of gathering data of high scientific merit, i.e. data of great importance to understanding the feature of interest, by deriving the sampling locations from a prediction of the evolution of a given feature of interest. We build upon the three-dimensional (two spatial dimensions plus time), single-vehicle algorithm presented in Smith et al. (2009a), with the intention of generating a mission plan that accurately steers multiple gliders to locations of high value within an evolving ocean feature. The primary contributions of this paper are the development of an innovative toolchain, and the waypoint-generation algorithms for the practical application of AUV path planning and trajectory design.

The goal of this study is to present an innovative ocean sampling method that utilizes model predictions and gliders to collect scientifically interesting oceanographic data that can also increase the predictive skill of a model. Our motivation is to track and collect daily information about an ocean process or feature which has a lifespan on the order of weeks. Based on the interesting biogeochemical ocean dynamics presented in Section 2, in addition to its proximity to our laboratories at USC, we choose to focus our research on an oceanographic region referred to as the Southern California Bight (SCB)[1]. The regional location of the SCB is denoted by the box in Figure 1(a), with an enlarged view of the SCB presented in Figure 1(b).

The mission plan to track and monitor dynamically evolving ocean processes or features is iteratively generated as follows. First, we identify a feature of interest in the SCB via direct observation or through remotely sensed data (e.g. satellite imagery). We then use a regional ocean model to predict the behavior of this feature, e.g. outfall from a waste water treatment plant, over a short time period, such as one day. This prediction is used to generate a sampling plan for deployed glider(s) that steer the vehicle(s) to regions of scientific interest, based upon the given feature and its predicted evolution. Throughout execution of the sampling plan, collected data are transmitted via an embedded wireless network (Pereira et al. 2009; Smith et al. 2009b), and assimilated into the ocean model. Incorporating this *in situ* ground truth, a new prediction is generated by the model. This entire process is repeated until the feature dissipates or is no longer of interest.

We begin our discussion with a description of the primary research focus related to this study, a harmful algal bloom (HAB). An algal bloom, and in particular a HAB, is a rapid increase of biomass of phytoplankton or cyanobacteria (potentially toxin producing species) caused by the addition of nutrients to and/or an alteration in the chemical properties of the ocean. Nutrients can be added to the coastal ocean via river runoff or waste water outfalls. Ocean chemistry can be altered by the addition of freshwater from these events, as well as by ocean processes such as an eddy or upwelling.

We continue our discussion with definitions of the sensor platform and ocean model considered, and a review of previous work related to similar problems. Section 5 contains an in-depth discussion and statement of the path planning problem, and describes the two main algorithms designed to obtain the waypoints that define our path. Here we present a waypoint-selection algorithm for both a boundary-tracking and a centroid-tracking mission scenario. We design sampling plans and present simulated and implemented experimental results for AUV retasking in Southern California coastal waters. We conclude with an analysis of the experimental results and present areas of ongoing and future investigation. A crucial component to this study is the validation of this toolchain via at-sea trials. Extensive deployment time ($> 1,500$ km traversed
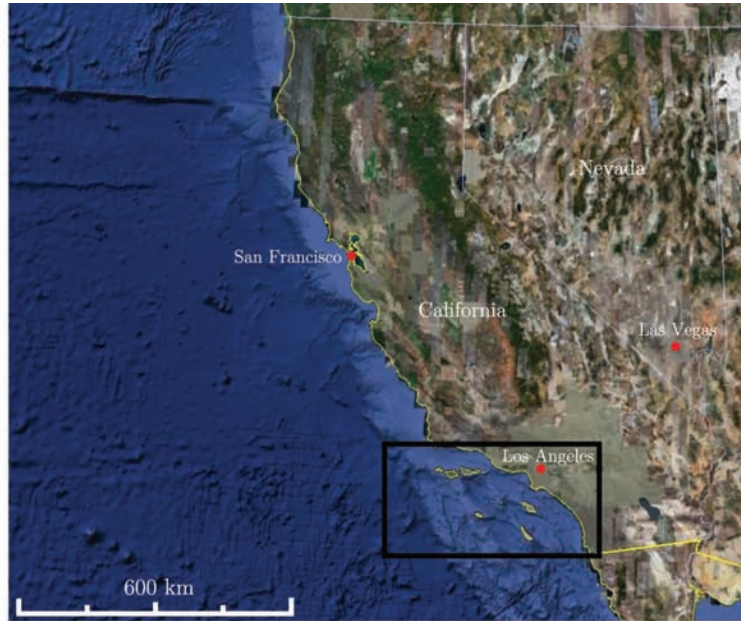
(a)
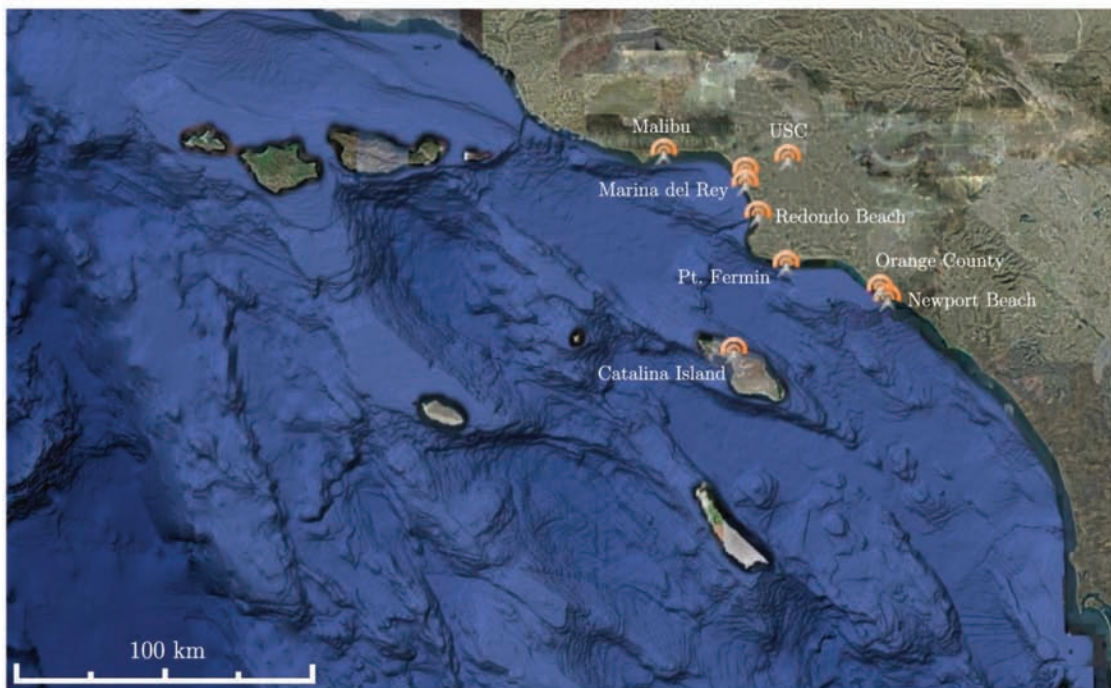
(b)

Fig. 1. (a) Google Earth image of the state of California. The oceanic region contained in the rectangle denotes the Southern California Bight. An enlarged image of the Southern California Bight is presented in (b). The Southern California Bight is the oceanic region contained within $32°$ N to $34.5°$ N and $-117°$ E to $-121°$ E. This region is the primary area of interest, investigation and deployment for the USC CINAPS team. The labeled orange arcs are the locations of the base stations that compose the wireless sensor network presented in Smith et al. (2010a).

during more than 100 days at sea from January 2009 to September 2009) has provided several successful validation results. Here we present two examples of feature-tracking missions implemented on deployed gliders.

2. Background and Motivation

2.1. Southern California Ocean Dynamics

The motivation for using predictive capabilities to design trajectories with the intent of tracking an evolving ocean feature is derived from a practical problem that exists in many coastal communities around the world, and, in particular, Southern California. As the rate of urbanization in coastal communities continues to increase, land use and land cover (i.e. significant increase in impervious surfaces) in these areas are permanently altered. This alteration affects both the quantity of freshwater runoff, and its particulate and solute loadings, which has an unknown impact (physically, biogeochemically, biologically and ecologically) on the coastal ocean (Warrick and Fong 2004). One documented result of these impacts is an increase in the occurrence of algal and phytoplankton blooms. Such biological phenomena are a primary research interest of the authors. In particular, we are interested in the assessment, evolution and potential prediction of algal blooms that have the potential to include harmful algal species (i.e. harmful algal blooms (HABs)). The environmental triggers leading to the onset, evolution and dissemination of HAB events are widely unknown and are under active investigation.

Given the ecological and socio-economic importance of coastal regions, like Southern California (U.S. Commission on Ocean Policy 2004), it is important to be able to accurately assess, and ultimately predict, how changes driven by urbanization and climate impact these areas.

In addition to regional anthropogenic disturbances, Southern California experiences significant decadal and interannual variability associated with the Pacific decadal oscillation (PDO) and the El Niño southern oscillation (ENSO) (Dailey et al. 1993; Kennedy et al. 2002). These climatic phenomena impact the frequency and intensity of the regional episodic storm events, as well as the physical and biogeochemical dynamics of the coastal marine ecosystem. The increased rainfall in an urban, coastal region results in freshening of sea-surface waters through direct rainfall into the ocean and from freshwater inflow at the coastal boundary from streams and rivers. The river runoff supplies nutrient-rich waters to the ocean surface, which may lead to a *bloom* of photosynthetic organisms (i.e. algal bloom).

An open question in coastal ocean science is to disseminate whether or not we can distinguish anthropogenically affected processes from natural variations and effects. The ability to track and monitor evolving features resulting from anthropogenic inputs can help answer this question and others related to the increased urbanization of coastal regions.

2.2. Harmful Algal Blooms

Microscopic organisms are the base of the food chain and are what all aquatic life ultimately depends upon for food. There are a few dozen species of phytoplankton and cyanobacteria that can create potent toxins when provided with the right conditions. These harmful algae can cause harm via toxin production, or by their accumulated biomass which may affect levels of dissolved oxygen in the water. Impacts to humans from HABs include, but are not limited to, severe illness and potential death following consumption of, or indirect exposure to, HAB toxins. In addition, coastal communities and commercial fisheries can suffer severe economic losses due to fish, bird and mammal mortalities, and decrease in tourism due to beach closures. For these reasons, it is of interest to predict when and where HABs may form and which coastal areas they may affect. For general information on HABs, we refer the interested reader to Anderson (2008). Harmful algal blooms are an active area of research on all coasts of the United States, and are of large concern for coastal communities in Southern California (Schnetzer et al. 2007).

A related threat of HABs deals with the sinking of *Pseudonitzschia*, i.e. transfer of toxicity to the sea floor, as discussed in Wood et al. (2009). Autonomous gliders have been used recently during the North Atlantic Bloom experiment to track the sinking of primary production from the surface to 800–1,000 m (Gray et al. 2008). It is of interest to document the sinking of the *Pseudonitzschia* biomass to determine the harmful effects away from the surface. Vertical movement or aggregation at specific depths can also be important factors affecting the abundance of some harmful algae such as dinoflagellates and their associated toxins (Kudela et al. 2008). Marine biologists are interested in defining the vertical zonation and migratory patterns of a dinoflagellate, and the interactions of the organism with physical processes of the ocean (e.g. currents, shear, density gradients, light) and the chemical structure (e.g. nutrients). Hence, with their unique sawtooth-shaped trajectories, gliders are a good candidate platform to study surface blooms as well as their vertical migration.

Motivated by the number of problems linked to HABs, and algal blooms in general, it is of interest to study ocean features that can potentially promote a bloom event. In particular, blooms are likely to occur when nutrient-rich waters are brought to the surface. Ocean processes and features of interest promoting these conditions are cold-core eddys, upwelling, river runoff and waste water outfalls. These events alter the biochemical composition of the surrounding water, and provide the excess nutrients to support higher productivity and a *bloom* of microorganisms.

From the coastal dynamics and rapid urbanization in Southern California coastal communities discussed earlier, we choose *plumes* from river runoff and waste water outfalls as features to track and monitor. Both of these events can be discretely quantified; river runoff happens after a storm event and most waste water outfalls are human controlled. Hence, we have a good idea of when and where a plume will be present in the SCB, and can employ the proper means to detect its onset and evolution. Henceforth, we will refer to a feature of interest to be tracked as a *plume*, which is

understood to encompass freshwater plumes, waste water outfalls and algal blooms.

The density of the considered plumes is less than the surrounding sea water, and forms a lens on the surface. The movements of these plumes are dominated by surface currents and local winds. The focus of this paper is on tracking the movement of plumes through the ocean by use of predictive tools and gliders to study the factors and conditions leading to the onset and lifespan of a HAB event. We remark that similar techniques to those presented here can be applied to study eddys and upwelling; however, with the choice taken here, we increase the likelihood of catching an actual event upon which to implement this innovative technology toolchain and trajectory design method.

3. Regional Ocean Modeling System

The predictive tool utilized in this study is the regional ocean model system (ROMS) – a split-explicit, free-surface, topography-following-coordinate oceanic model. ROMS is an open-source, ocean model that is widely accepted and supported throughout the oceanographic and modeling communities. Additionally, the model was developed to study ocean processes along the western U.S. coast, which is our primary area of study. The model solves the primitive equations using the Boussinesq and hydrostatic approximations in vertical sigma (i.e. topography-following) and horizontal orthogonal curvilinear coordinates. ROMS uses innovative algorithms for advection, mixing, pressure gradient, vertical-mode coupling, time stepping and parallel efficiency. Detailed information on ROMS can be found in Shchepetkin and McWilliams (1998, 2005).

The version of ROMS used in this study is compiled and run by the Jet Propulsion Laboratory (JPL), California Institute of Technology, and provides hindcasts, nowcasts and hourly forecasts (up to 36 h) for the SCB via a web interface (Vu 2008) or via access to their THREDDS data server (Jet Propulsion Laboratory 2009). The JPL version of ROMS (see e.g. Chao et al. (2008) and Li et al. (2008a,b)) assimilates HF radar surface current measurements, data from moorings, satellite data and any data available from sensor platforms located or operating within the model boundary.

This model utilizes a nested configuration, with increasing resolution covering the U.S. western coastal ocean at 15 km, the Southern California coastal ocean at 5 km and the SCB at 1 km. In addition to the 1 km output, a resampled 2.2 km resolution output, correlated to the assimilated HF radar grid resolution, is produced. The computations and predictions presented here use this 2.2 km resolution product.

The interaction with JPL related to this research and ROMS improvement is a two-way street. We need the predictions to design efficient, effective and innovative

Fig. 2. One of the two Slocum gliders owned and operated by CINAPS. The glider has just been deployed and is preparing to start a mission. This picture was taken directly north of the entrance to Isthmus Cove off the northeast coast of Santa Catalina Island.

AUV trajectories. The JPL updates their ROMS by utilizing the feedback from field deployments to assess the validity of each prediction, and to increase the skill of future predictions.

4. Mobile Sensor Platform: AUV

The mobile sensor platforms used in this study are Webb Slocum autonomous underwater gliders (Webb Research Corporation 2008); see Figure 2. A glider is a type of AUV designed for long-term ocean sampling and monitoring (Schofield et al. 2007). These gliders *fly* through the water by altering the position of their center of mass and changing their buoyancy. Due to this method of locomotion, gliders are not fast-moving AUVs, have operational velocities on the same order of magnitude as oceanic currents ($\backsim 1$ km h^{-1}) and follow a sawtooth-shaped trajectory. The endurance ($\backsim 1$ month per deployment) and velocity characteristics of a glider make it a good candidate vehicle to track plumes that move with ocean currents, and that have a residence time on the order of weeks. We have upgraded the communication capabilities of our gliders to take advantage of, and become, a node in our local wireless network; details can be found in Pereira et al. (2009) and Smith et al. (2009b).

Considerable work has been done on the kinematic and dynamic modeling and control of underwater gliders, and we refer the interested reader to Leonard and Graver (2001), Graver (2005) and the references therein for a detailed treatment of these topics. Here we assume that the glider

can successfully navigate from one location to another. This is a non-trivial assumption due to the complexity of the underwater environment and the forces experienced by an AUV while underway. An entire body of research exists that is dedicated to accurate and precise execution of prescribed missions by AUVs, and is outside the scope of the work presented here. In relation to this work, research is active to improve the navigational accuracy of our gliders by use of ROMS predictions in the SCB; see Smith et al. (2010b,c).

Briefly, an example mission for a standard glider consists of a set maximum depth along with an ordered list of geographical waypoints $(W_1, \ldots, W_n)$. An exact path or trajectory connecting these locations is not prescribed by the operator, nor are the controls to realize the final destination. When navigating to a new waypoint, the present location L of the vehicle is compared with the next prescribed waypoint in the mission file (W_i), and the on-board computer computes a bearing and a range for execution of the next segment of the mission. We will refer to the geographical location at the extent of the computed bearing and range from L to be the aiming point A_i. The vehicle then dead reckons with the computed bearing and range towards A_i with the intent of surfacing at W_i. The glider operates under closed-loop heading and pitch control only. Thus, the computed bearing is not altered, and the glider must surface to make any corrections or modifications to its trajectory. When the glider completes the computed segment (i.e. determines that it has traveled the requested range at the specified bearing), it surfaces and acquires a GPS fix. Regardless of where the vehicle surfaces, waypoint W_i is determined to be *achieved*. The geographical positional error between the actual surfacing location and W_i is computed, and any error between these two is fully attributed to environmental disturbances (i.e. ocean currents). A depth-averaged current vector is computed, and this is considered when computing the range and bearing to W_{i+1}, the next waypoint in the mission list. Hence, A_i is in general not in the same physical location as W_i. The offset between A_i and W_i is determined by the average velocity and the perceived current experienced during the previous segment.

5. Problem Outline and Path Planning

In this section, we formally pose the path planning problem and present the algorithms that generate the locations (waypoints) for the AUV to visit, which steer it to follow the general movements of a plume. Depending upon the feature considered, and the instrumentation suite available on the vehicle, different locations within a feature may be of interest, e.g. its boundary or extent, subsurface chlorophyll maximum, salinity minimum, its centroid, O_2 or CO_2 threshold, etc. Since the focus of this research is on asset allocation to the *right place at the right time*, and is only motivated by the study of HABs in the SCB, we choose to track proxy areas of interest within a given feature. In

particular, we extend the work presented in Smith et al. (2009a) to include the use of multiple vehicles to track the centroid and the boundary of the extent of a plume. Similar algorithms to those presented here are under development, and will consider alternate sampling locations, such as the aforementioned areas of interest.

Considerable study has been reported on adaptive control of single gliders and coordinated multi-glider systems; see e.g. Paley et al. (2007, 2008) and the references therein. In these papers, the trajectories given to the gliders were fixed patterns (rounded polygons) that were predetermined by a human operator. The adaptive control component was implemented to keep the gliders in an optimal position, relative to the other gliders following the same trajectory. The difference between the method used in Paley et al. (2008) and the approach described here is that our sampling trajectory is determined from the output of ROMS, and, thus, at first glance, may appear as a seemingly random and irregular sampling pattern. Such an approach is a benefit to the ocean modelers and scientist alike. Scientists can identify sampling locations based upon ocean measurements they are interested in following, rather than setting a predetermined trajectory and hoping the feature enters the transect while the AUV is sampling. When deploying multiple vehicles, this method allows the operator to generate trajectories that survey an appropriate spatial extent of the feature of interest. And, model skill is increased by the continuous assimilation of the *in situ* collected data; which, by choice, is not a continuous measurement at the same location.

A plume may dissipate rapidly, but can stay cohesive and detectable for up to weeks. It is of interest to track these plumes based on the discussion in Section 2 as well as in Cetinic et al. (2010). In addition to tracking a plume, it is also important to accurately predict where a plume will travel on a daily basis. Such knowledge can aid in proper assessment for beach and fishery closures to protect humans from potential toxins of HABs occurring in the area. The ROMS prediction capabilities are good, but model skill can significantly increase from assimilation of *in situ* measurements. Since ROMS assimilates HF radar data for sea surface current measurements, we can make the general assumption that predicted surface velocities are fairly accurate. Also, assuming a no-slip boundary condition, the model is assumed accurate within a few meters of the sea floor. For the region between the top few meters and the bottom few meters, the ability to accurately predict ocean current velocity is highly debated, especially in near-shelf regions. Open-ocean, autonomous navigation is a challenging task, primarily due to the complexity of unknown environmental disturbances, such as ocean currents. For most of the ocean, we only have a general notion of the variability of current velocity as a function of both depth and time. ROMS provides a prediction of this variability that can be leveraged for AUV navigation. A long-term effort of this research is to address the open question of how beneficial ocean model predictions are for

increasing the accuracy and effectiveness of path planning and trajectory design for AUVs.

Currently, commercially available, remote-sensing technologies for ocean observation only allow us to extract information from the first few meters of the upper water column. Large-scale detection of ocean features, e.g. algal blooms, existing more than a few meters below the surface is not possible at this time. Only through ship-side sampling or driving a mobile sensor through the feature can we extract any information regarding its 3-D structure. Since ship sampling is time consuming, expensive and infrequent, and steering a mobile asset to a precise location for sampling is very difficult, we have a great deal to learn about the 3-D structure and evolution of algal blooms. In addition to the the physical structure and composition, the drivers and mechanistic processes behind bloom conception, evolution and collapse are not well understood due to complex interactions between the members of the microbial communities and the surrounding environment. As a result, our capacity to assess the range of potential future scenarios for a plume that might result is highly limited. To this end, and as an initialization point for this area of research, we choose to track features that are observable via commercial remote-sensing techniques, or direct observation. This choice presents us with a 2-D representation of the feature extent, although it is known that this observed feature has some 3-D structure that we would like to investigate. Since the feature will propagate and evolve with ocean currents and internal microbial interactions, it is of interest to utilize a mobile sensor, e.g. glider, to track the feature to gather time-series data from within and around the feature. In this paper, we assume that ocean currents dominate the propagation of the given feature. Since our initial representation of the feature is 2-D and on the ocean surface, we assume that the plume is propagated primarily by ocean surface currents, which, as previously mentioned, have fairly accurate predictions from ROMS. The waypoint-selection algorithms presented in Section 5.2 that determine the path for the glider are based on the 2-D propagation predictions. By implementing these paths on gliders, which traverse the ocean following a sawtooth trajectory, we hope to gain more information about the 3-D structure and evolution as the glider samples vertically through the water column.

With the development of a new technology or innovation, it is important to assess the associated strengths and weaknesses. For implementation of AUVs to conduct ocean observation, there are a few established methods for path planning and trajectory generation, e.g. lawnmower pattern, transect lines or a regular grid, with which to compare new approaches. However, these techniques are not known to be optimal or even efficient for a given ocean sampling mission. Additionally, the metric of success for the paths executed by these vehicles may not be linked to optimization of some cost, but is primarily dependent upon the data collected during the deployment. A regular grid pattern placed in the appropriate location may be an excellent option (see e.g. Das et al. (2010)),

but may also entirely miss an evolving algal bloom hot spot. In our method, we choose to try to keep the vehicle moving with the feature, to increase information gain, and decrease the potential for the feature to outrun the vehicle. Accurately assessing and comparing the effectiveness of the path planning techniques presented here is a task for a multi-year, multi-deployment study, in which sampling techniques are implemented simultaneously to study the same feature of interest. We are working towards implementing a system to determine the environmental triggers for onset, development and ultimate mortality of an algal bloom. Thus, we are motivated to track algal blooms or features that have the potential to become algal blooms, and develop efficient strategies to keep the sensor within the feature for as long as possible to gather data that will help us understand more about these complex phenomena.

5.1. Problem Statement

Given a plume, we are interested in designing trajectories to guide autonomous gliders to track and sample along the path of the centroid, as well as the boundary or extent. We will assume that we have at least two vehicles to perform the missions, e.g. one centroid tracker and one boundary tracker. Due to the large amounts of chromophoric dissolved organic matter, a plume resulting from river runoff or waste water outfall can easily be identified from satellite imagery with visible coloring on the ocean surface. Additionally, these directly follow a rain event, and the discharge location (i.e. river mouth) is well known or, in the case of waste water outfalls, is determined by the local sanitation district. Thus, we may assume that we are aware of the occurrence and can delineate the boundary or extent of a plume at an initial point in time. As previously mentioned, the plume boundary is a 2-D feature defined by the outline presented in remotely sensed satellite imagery using proxies, such as fluorescence line height (FLH) and chlorophyll. On-board the glider, chlorophyll and optical sensors, among others, collect data regarding specific properties of the water. The paths presented here are not adaptive during implementation, as restricted by the glider's operation, so we do not intend the vehicles to detect or sense the boundary of a plume during a mission. Data is collected and post-processed to examine dissipation, dispersion, chemical changes, etc. of the plume. These data are analyzed to further understand plume ecology and evolution, as well as to assess model predictions. Additionally, for the planning results presented here, we assume that the plume we are tracking is a single connected region. In all likelihood, a plume or algal bloom that we are interested in may evolve into multiple disconnected regions. In this case, we select a single region to track based on parameters of scientific interest. The choice of a particular region to track is ongoing work done by other members of our research team. For example, a region or *hot spot* can be chosen using the detection algorithm presented in Section IIB of Das et al. (2010), which is

based on thresholding FLH values from satellite imagery. Other proxies that may be used for selecting a region to track include chlorophyll-a and normalized water-leaving radiance at 551 nm ($L_{wN}(551)$), both detected via satellite imagery.

Since we assume that the propagation of the plume is determined primarily by surface currents, we forecast its hourly movement by use of ROMS surface current predictions; see Smith et al. (2009a). The prediction begins with the initial delineation of the plume and is the basis for determining the waypoints that define the computed paths. For safety concerns, we restrict a glider to surface no more than once every four hours. In Smith et al. (2009a), we considered surface intervals as short as one hour. However, surfacing that frequently kept the vehicle close to the surface and in danger of collision with other vessels[2]. In addition, upon surfacing the glider acquires a GPS fix, and communicates its position and collected data over the network. This communication time is significant ($\backsim$ 15 min) when considering the temporal aspect of tracking a moving plume. This gives further support for the restriction to a 4-h interval between surfacings because the more time the glider is on the surface, the less time it is collecting data and keeping up with the moving plume. The 4-h interval was chosen to reduce surfacings during a mission, but also to allow for frequent contact with the vehicle. Hence, in an instance of a severe modeling error, computational error or gross misguidance, we have the ability to abort, replan the mission and potentially get back on track. Since the basic idea is to track the plume for many days while assimilating collected data into the model, the accuracy of the model prediction degrades with time and we need time to run the model each day, we choose to plan a $T = 16$ h tracking and sampling mission for each day as early in the ROMS prediction as possible.

To begin, we assume that the starting location L of each vehicle is known, and the prediction of the plume evolution is accurate. The initial delineation of the plume is done by selecting a set of geographical locations ($\mathcal{D}$) that encompass the plume's extent. The discrete locations in $\mathcal{D}$ are forecasted as if they were Lagrangian drifters in the ROMS surface current prediction. Additionally, we assume that the glider travels at a constant speed v km h^{-1}, and define d_h km to be the distance (in kilometers) traveled in h h. For the waypoint selection and path generation, we do not consider vehicle separation except for guaranteeing that two vehicles are not sent to the exact same location at the exact same time. The gliders do not have the sensory capabilities to actively assess vehicle separation while underwater; thus, there is no way to enforce a separation constraint on a deployed glider, even if we imposed one during the path planning stage. There is no adaptive behavior incorporated during the execution of the planned trajectory. In particular, we do not provide an adaptive approach in our algorithm to overcome model or navigational error when tracking a plume. It is well known that an autonomous

glider is a slow-moving vehicle with limited control capabilities. With this in mind, if the vehicle surfaces in a location that is extremely off course, or conditions have changed dramatically, our remediation approach is to generate a new plan. The idea is to improve the collection of scientific data by predicting the best locations to send a glider to, while also providing feedback to JPL on the accuracy of ROMS. In the long run, both communities will benefit.

5.2. Waypoint-selection Algorithms

In this section, we present the centroid and boundary-tracking, waypoint-generation algorithms. These algorithms utilize the ROMS hourly predictions of a delineated plume to generate a sampling mission that guides the AUV to predicted locations of the selected areas of interest within the given feature. As previously mentioned, the areas of interest for a given feature may be different based upon the sensor suite available on the vehicle and/or the science return desired. The use of path planning to collect data of high scientific merit, with respect to a selected area of interest, translates to navigating the vehicle to a location that contains the quantity to be measured or area to be surveyed. Note that for both the implemented and simulated experiments presented in Sections 6 and 7, we neither consider vehicle dynamics nor the effect of the ocean currents upon the vehicle in the determination of the paths. The reasoning behind this omission is based in the initial study upon which this paper is based (Smith et al. 2009a). Our motivation was to develop high-level path planning techniques, and we made the assumption that a low-level controller was in place and was sufficient to steer the vehicle between two prescribed waypoints. Given that Slocum gliders are used widely in oceanographic applications, and are proven to be very robust platforms, this assumption seemed reasonable, and we were willing to initially accept navigational errors based on the standard operation of the chosen test-bed platform during the preliminary stages of this research. Over the last year, we have conducted several field trials with multiple gliders, traversing > 1500 km over > 100 days at sea. From these deployments, we have compiled a database to analyze the navigational accuracy of the gliders and their ability to realize a prescribed path. Considering more than 200 trajectories, with an average distance traveled of 2 km, the median error between the actual location where a glider surfaced and the prescribed surfacing location was 1.1 km. Details of this analysis are presented in Smith et al. (2010c). Based on this analysis, it was determined that we needed to increase the accuracy of the gliders to effectively execute the paths computed by use of the algorithms presented here. This is especially the case when attempting to design a strategy to steer a vehicle to a specific location within an evolving feature. To this end, we have developed extensions to the waypoint-selection algorithms presented here that incorporate

4-D (three spatial plus time) velocity predictions into the trajectory design of the glider (Smith et al. 2010c). Here we present preliminary results that show a 50% reduction in navigational error by using ROMS predictions, rather than the depth-averaged current estimations utilized for standard glider operations. Additionally, research is ongoing to couple vehicle kinematics and dynamics with ocean current predictions to generate trajectories to follow the paths that track evolving ocean features; see Smith et al. (2010b) for preliminary results.

5.2.1. Centroid-tracking Algorithm We begin with the centroid-tracking, waypoint-generation algorithm. Let $T \in \mathbb{Z}^+$ be the duration, in hours, of the planned mission. The input to the trajectory design algorithm is a set of points, $\mathcal{D}$ (referred to as drifters) that determine the initial extent of the plume ($\mathcal{D}_0$), and hourly predictions ($\mathcal{D}_i$, $i \in T$) of the location of each point in $\mathcal{D}$. For the points in $\mathcal{D}_i$, we compute the convex hull as the minimum bounding ellipsoid, E_i, for $i \in T$. We consider the predicted locations of $\mathcal{D}_0$ after 4 h, $\mathcal{D}_4$. We let C_i be the centroid of E_i, and, with a slight abuse of notation, also refer to C_i as the centroid of $\mathcal{D}_i$. The algorithm computes $d_g(L, C_4)$, where $d_g(x, y)$ is the geographical distance from x to y. Given upper and lower bounds d_u and d_l, respectively, we have three possible cases for choosing a location to send the glider to. Case 1: if $d_l < d_g(L, C_4) \leq d_u$, the generated waypoint is C_4, and the path is simply defined as the line $\overline{LC_4}$; see Figure 3(a). Case 2: if $d_g(L, C_4) \leq d_l$, the algorithm first checks to see if there exists a point $p \in E_4 \cup \mathcal{D}_4$ such that

$$d_l \leq d_g(L, p) + d_g(C_4, p) \leq d_u. \tag{1}$$

If such a point exists, the algorithm generates two waypoints (p and C_4) and the path is defined as the line $\overline{Lp}$ followed by the line $\overline{pC_4}$. In general, this will not be the case, since the distance from the centroid of the plume to its boundary can be many kilometers. Thus, if $\{p \in E_4 \cup \mathcal{D}_4 | d_l \leq d_g(L, p) + d_g(C_4, p) \leq d_u\} = \emptyset$, then the algorithm computes the locus of points, $\mathcal{L} = \{p^* \in \mathcal{L} | d_g(\mathcal{L}, p) + d_g(p, C_4) = d_4\}$, and selects a point at random, $p^* \in \mathcal{L}$, as another waypoint. Here the path is the line $\overline{Lp^*}$ followed by the line $\overline{p^*C_4}$; see Figure 3(b). This additional waypoint computation was inserted into the algorithm when considering a single-vehicle deployment. In this scenario, one would like to acquire as much data as possible. In the case of a multiple-vehicle mission, it is less useful to include the additional waypoint in the trajectory design, as the other vehicles are gathering supplemental data. During deployment, p^* is visited if and only if we feel the safety of the vehicle will not be compromised by frequent surfacings (e.g. based on geographical location, day of the week and time of day). Case 3: if $d_g(L, C_4) > d_u$, the algorithm generates a waypoint C_w in the direction of C_6, such that $d_g(L, C_w) = d_4$; see Figure 3(c). The choice of C_{i+6} over C_{i+j}, $j \in \{5, 7, 8\}$, is made here since C_{i+6} is the predicted location of the centroid halfway between the

surface interval times. Here we choose C_{i+6} to be fixed for all scenarios, and, as in Smith et al. (2010c), we incorporate $C_{i+j}, j \in \{5, 6, 7, 8\}$, as an optimization parameter to give the glider the best chance of executing the prescribed path. Let $AZ(a, b)$ be the azimuth angle between locations a and b. The location of the vehicle L is updated to C_4 or C_w and the process is iterated for the duration T. This waypoint-generation process is presented in Algorithm 1.

Algorithm 1 Centroid-tracking, Waypoint-selection Algorithm

Require: Hourly forecasts, $\mathcal{D}_i$, for a set of points $\mathcal{D}$ defining the initial plume condition and its movement for a period of time, T.
  for $0 \leq i \leq T$ **do**
    Compute C_i, the centroid of the minimum bounding ellipsoid E_i of the points $\mathcal{D}_i$. Compute d_4.
  end for
  while $0 \leq i \leq T - 1$ **do**
    if $d_l \leq d_g(L, C_{i+4}) \leq d_u$ **then**
      The trajectory is $\overline{LC_{i+4}}$.
    else if $d_g(L, C_{i+4}) \leq d_l$ and $\exists p \in E_{i+4} \cup \mathcal{D}_{i+4}$ such that $d_l \leq d_g(L, p) + d_g(p, C_{i+4}) \leq d_u$ **then**
      The trajectory is $\overline{Lp}$ followed by $\overline{pC_{i+4}}$.
    else if $d_g(L, C_{i+4}) \leq d_l$ and $\{p \in E_{i+4} \cup \mathcal{D}_{i+4} | d_l \leq d_g(L, p) + d_g(p, C_{i+4}) \leq d_u\} = \emptyset$ **then**
      Compute $\mathcal{L} = \{p^* \in \mathcal{L} | d_g(L, p) + d_g(p, C_4) = d_4\}$, select a random $p^* \in \mathcal{L}$ and define the trajectory as $\overline{Lp^*}$ followed by $\overline{p^*C_{i+4}}$.
    else if $d_g(C_i, C_{i+1}) \geq d_u$ **then**
      Compute C_w such that $d_g(l, C_w) = d_4$ and $AZ(L, C_w) = AZ(L, C_6)$.
    end if
  end while

5.2.2. Boundary-tracking Algorithm Similarly to the presentation in Section 5.2.1, we define the boundary-tracking, waypoint-generation algorithm, presented in Algorithm 2. We begin with the same predictions as above, and define P_i to be the polygon formed by connecting the points $\mathcal{D}_i$ for $i \in T$. Let $B(a, r)$ be the disc of radius r, about a. This algorithm first computes $N = B(L, d_4) \cap P_4$. Again we have three possible cases to investigate to define the path for the boundary-tracking vehicle. Case 1: if $N \geq 2$, the generated waypoint B_4 is a random selection of one of the intersection points; see Figure 4(a). Case 2: if $N = 1$, the generated waypoint B_4 is that precise intersection point; see Figure 4(b). Case 3: if $N = \emptyset$, B_4 is computed such that $d_g(L, B_4) = d_4$ and $AZ(L, B_4)$ is the average azimuth of $\mathcal{D}_i$ for the considered 4-h time period; see Figure 4(c). We reassign $L = B_4$, and the algorithm is repeated. For the boundary-tracking scenario, it would be of interest to traverse the entire predicted extent of the given plume over the duration of the survey. However, the test-bed vehicles considered move too slowly to entertain this sampling
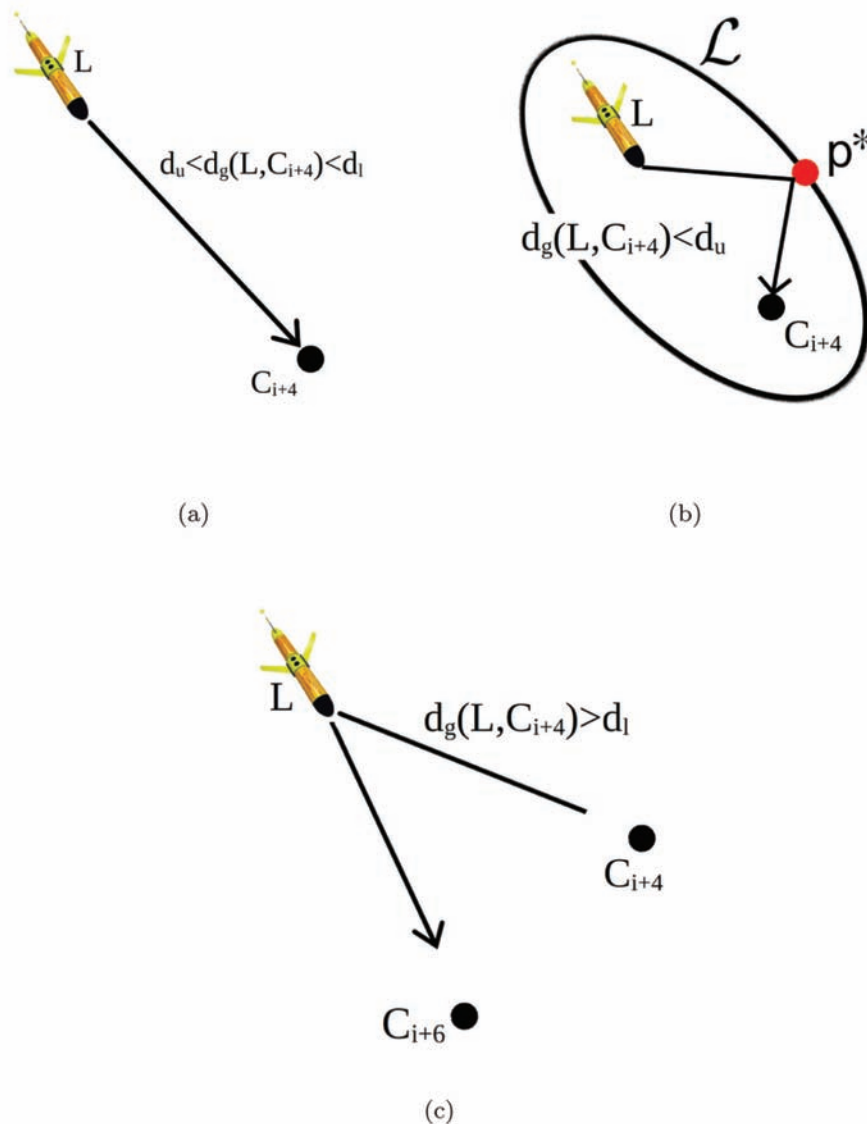
Fig. 3. The three possible cases for the waypoint generation that defines the path for the centroid-tracking vehicle. (a) Case 1: the distance from L to the predicted centroid C_4 is within the defined bounds, $d_l < d_g(L, C_4) \leq d_u$, and thus it is reachable. The generated waypoint is C_4, and the path is defined as the line $\overline{LC_4}$. (b) Case 2: the distance from L to the predicted centroid C_4 is less that the defined lower bound, $d_g(L, C_4) \leq d_l$, so the algorithm computes an additional waypoint, p or p^*, to be visited. The path is the line $\overline{Lk}$ followed by the line $\overline{kC_4}$, for $k \in \{p, p^*\}$. (c) Case 3: the distance from L to the predicted centroid C_4 is greater than the defined upper bound, $d_g(L, C_4) > d_u$; thus, it is determined to be unreachable. Here the algorithm defines a waypoint C_w, such that $d_g(L, C_w) = d_4$ and $AZ(L, C_w) = AZ(L, C_6)$. The path is defined as the line $\overline{LC_w}$.

method. Thus, we choose to select a random point on the boundary when posed with multiple options. Also, since we are interested in assessing the dispersion, and potentially the subsurface mixing of the plume waters with the surrounding ocean waters, navigating near or crisscrossing the actual plume boundary can gather interesting data.

5.2.3. Ocean Plume Tracking Algorithm Based on Ocean Model Predictions After we have generated the waypoints that define the trajectory for the vehicle to follow, we

implement an iterative procedure to track the feature of interest over multiple days. This involves assimilating gathered data into ROMS and updating the projections for generating the trajectories for subsequent days. This overall iterative process to design an implementable plume tracking strategy based on ocean model predictions is given in Algorithm 3. With the inclusion of the optimization parameter mentioned in Section 5.2.1 and the incorporation of the 4-D ROMS current predictions in determining the path between the selected waypoints, Algorithm 3 has been
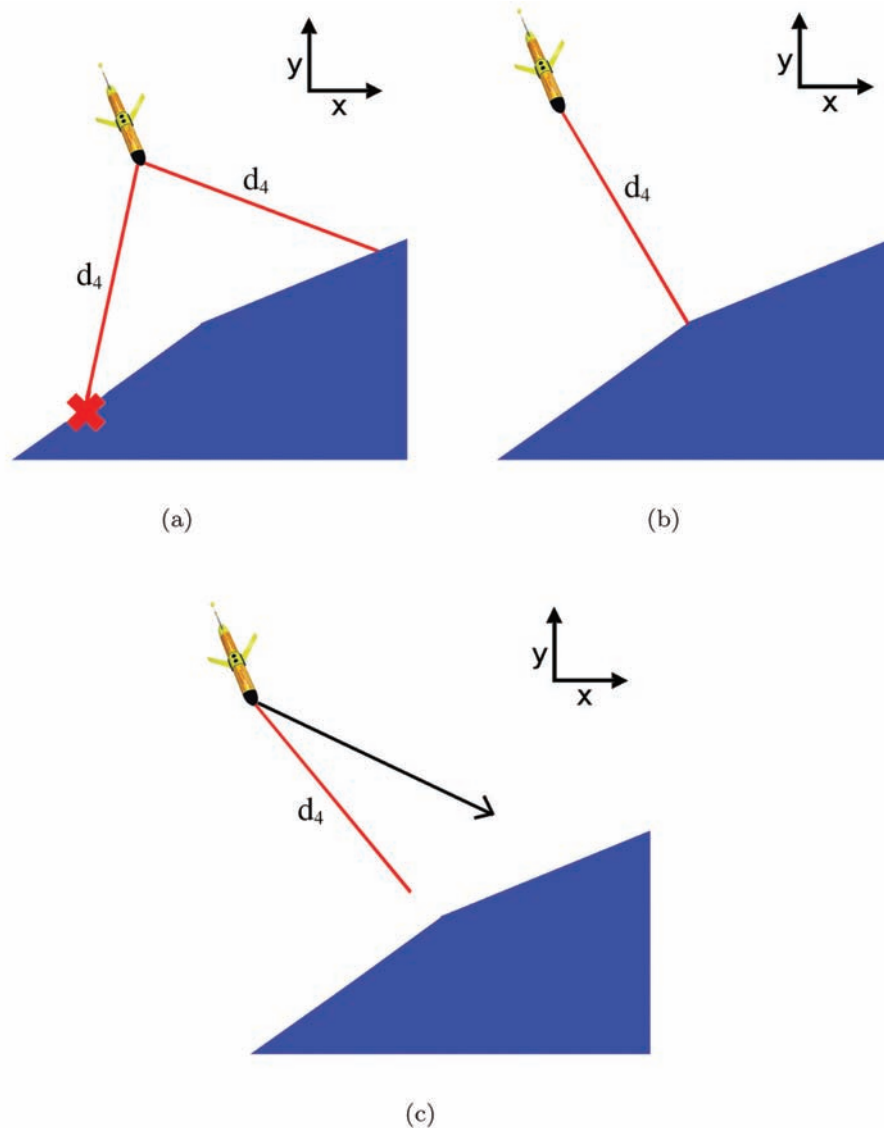
Fig. 4. The three possible cases for the waypoint generation that defines the path for the boundary-tracking vehicle. (a) Case 1: a circle of radius d_4 about L intersects the predicted polygon that defines the boundary of the plume, P_4, at least twice, $N \geq 2$. The generated waypoint B_4 is a random selection of one of these intersection points, and the path is defined as $\overline{LB_4}$. (b) Case 2: a circle of radius d_4 about L intersects the predicted polygon that defines the boundary of the plume, P_4, exactly once, $N = 1$. The generated waypoint B_4 is the intersection point, and the path is defined as $\overline{LB_4}$. (c) Case 3: a circle of radius d_4 about L does not intersect the predicted polygon that defines the boundary of the plume, P_4, $N = \emptyset$. The generated waypoint B_4 is computed such that $d_g(L, B_4) = d_4$ and $AZ(L, B_4)$ is the average azimuth of $\mathcal{D}_i$ for the considered 4-h time period, and the path is defined as $\overline{LB_4}$.

extended in Smith et al. (2010c), and is renamed the ocean plume tracking algorithm built on ocean model predictions (OPTA-BLOOM-Pred).

In the following sections, we proceed to present simulation and field experiments that implement paths generated by use of Algorithm 3. By construction, these paths are generated to track a plume that propagates on the ocean surface (0–30 m), while the vehicle used to track them, i.e. a Slocum glider, operates from the surface down to depths of $\sim$ 80 m. It is not valid to assume that

both of these are subjected to the same current regime, in both velocity and direction. In particular, a vertical velocity profile of ocean current for a given location within the SCB is, in general, not constant. This observation is illustrated in Figure 5 with an example plot of current velocity versus depth. Figure 5 displays a ROMS prediction for the meridional component of a vertical current profile located at 33.58° N, −118.38° E for 8 July 2009. From this example, we see that it may be possible for a plume to *outrun* a slow-moving vehicle (i.e. $d_g(C_i, C_{i+1}) \geq d_u$ or

Algorithm 2 Boundary-tracking, Waypoint-selection Algorithm

Require: Hourly forecasts, $\mathcal{D}_i$, for a set of points $\mathcal{D}$ defining the initial plume condition and its movement for a period of time, T.

    for $0 \leq i \leq T$ **do**

        Compute P_i, the polygon formed by connecting the points $\mathcal{D}_i$. Compute d_4.

    end for

    while $i \in \{4, 8, 12, 16\}$ **do**

        $j = i/4$

        if $B(L, d_4) \cap P_i \geq 2$ **then**

            B_j is one of the intersection points chosen at random. $L = B_j$.

        else if $B(L, d_4) \cap P_i = 1$ **then**

            B_j is the precise intersection point. $L = B_j$.

        else if $B(L, d_4) \cap P_i = \emptyset$ **then**

            $B_j = \{p | d(L, B_j) = d_4, AZ(L, B_j)$ is the average azimuth of $\mathcal{D}_i$ for $i = j - 4, \ldots, j\}$. $L = B_j$.

        end if

    end while

Algorithm 3 Ocean Plume Tracking Algorithm Based on Ocean Model Predictions

Require: A significant freshwater plume is detected via direct observation or remotely sensed data such as satellite imagery.

    repeat

        A set of points $(\mathcal{D})$ is chosen which determine the current extent of the plume.

        Input $\mathcal{D}$ to ROMS.

        ROMS produces an hourly forecast for all points in $\mathcal{D}$. Input hourly forecast for $\mathcal{D}$ into the trajectory design algorithms.

        Execute the trajectory design algorithms (Algorithms 1 and 2).

        Uploaded computed waypoints to the AUV.

        AUV executes mission.

        The AUV sends collected data to ROMS for assimilation into the model.

    until Plume dissipates, travels out of range or is no longer of interest.

$N = \emptyset$), especially when plumes may be propagated by surface currents driven by high winds that are typical during rain events in Southern California. Also, we remark that for a high-endurance, slow-moving vehicle like a glider, which generally will not have on-board instrumentation to measure current velocities *in situ* , e.g. an Acoustic Doppler Current Profiler (ADCP), having access to vertical current profile predictions can assist in areas of path planning, such as minimizing transit cost by staying in water masses that are moving in a preferred direction, or determining

unreachable areas due to large-magnitude currents. An extension of Algorithm 3 presented in Smith et al. (2010c) takes a step towards addressing the issue of incorporation of vertical distribution of current velocity into trajectory generation for AUVs.

6. Simulation

Multiple environmental agencies, local and regional policy makers, universities and outreach groups in Southern California collaborate together to assess the status of streams, estuaries, beaches and marine environments in Southern California. More than 90 local organizations contribute to this biannual effort called the Southern California Bight Regional Marine Monitoring Program, which includes assessment in areas of coastal ecology, water quality, rocky subtidal, areas of special biological significance and shoreline microbiology. Conducting large-scale, collaborative, regional assessments is a benefit to all agencies due to the widespread appeal and shared data products between all contributors. Rather than making comparisons to a small number of control sites, agencies are able to compare local results to the entire breadth of natural variability inherent to the ecosystem. This allows regulators to target resources where action is most needed. A few main questions posed for the study are the percentage of the Southern California mainland shelf area exhibiting signs of human disturbance, the number of stream miles impacted by anthropogenic activities, or the long-term effects of rapid urbanization in Southern California related to the frequency of occurrence of HAB events.

The next Southern California Bight Regional Marine Monitoring Program, commonly referred to as Bight 2010, is occurring from late-January through early-April 2010. The CINAPS group at USC will be a contributor in the Bight 2010 survey. One planned aspect of our contribution will be continuous operation of four Slocum gliders in the SCB for the entire three-month program. During this time, we are planning to implement the techniques presented in this work to retask currently operating gliders in the field to track and monitor a freshwater plume, waste water outfall or HAB event. Through careful planning and a bit of luck, we hope to capture the conditions in the SCB leading up to and development of a HAB event. To this end, we present a simulation experiment with four gliders tracking a feature of interest off the coast of Newport Beach, CA. The general area for the simulation is shown in Figure 6(a).

In this scenario, we offset the start times of the four vehicles to emulate asynchronous surfacing and communication with the vehicles or to simulate deploying the vehicles at multiple locations for the specific feature of interest. Deploying vehicles or sensors specifically for an event has the advantage of being able to place the sensor assets intelligently, or in a predetermined location, to best track the evolving feature. However, the disadvantage is that a vehicle is not collecting data if it is sitting on shore,
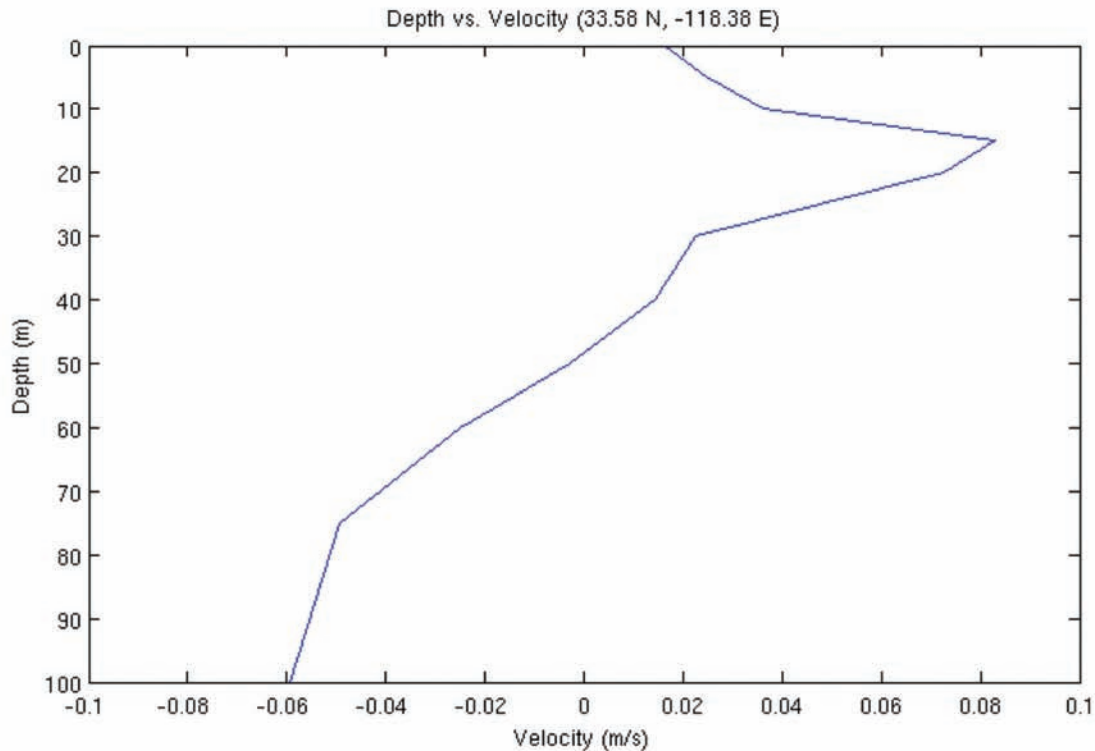
Fig. 5. An example vertical current profile prediction for a location within the SCB. This is a ROMS prediction of ocean depth versus current velocity for the meridional component located at 33.58° N, −118.38° E. This is a prediction made for 8 July 2009.

and important aspects of algal bloom development and evolution may be missed. Additionally, events occurring on shorter time scales may be entirely missed, as deployments do not always go as planned. For the features of interest considered in this study, even *intelligent* deployment can be non-trivial. As an example, consider the difference between a freshwater river runoff plume and a subsurface effluent algal bloom. Freshwater river outfall plumes are buoyant, and float high in the water. In general, these plumes have a stronger leading edge, i.e. sharper gradient, and a more diluted trailing edge. Thus, deploying gliders at the *front* of the plume may provide more information and allow the vehicle a better chance to remain in contact with the feature. For an algal bloom, it is a bit more complicated, as the boundary of the bloom is dependent on the kind of system that it is embedded in. In particular, subsurface effluent plumes are submerged, and become density equilibrated, making the boundary of the bloom more difficult to discern. Also, contrary to a freshwater plume, an algal bloom is composed of living organisms, whose life-cycle dynamics affect the movement and structure of the bloom in addition to the ocean currents. These chemical and biological dynamics, along with the 3-D composition and evolution of an algal bloom, are poorly understood, and are a primary motivation for developing techniques to place mobile sensors in the *right place at the right time* to gather data that will increase our understanding of these complex systems.

For the simulation, at $T = 0$ h, we deploy two vehicles, one centroid tracker and one boundary tracker, at the southern extent of the plume (predicted plume front). At $T = 2$ h we deploy a boundary-tracking vehicle on the predicted western boundary of the plume. Finally, at $T = 4$h, we start a boundary-tracking vehicle at the predicted northern boundary of the plume (predicted trailing edge of the plume). The initial delineation and location of the first two gliders are presented in Figure 6(a). The evolution of the plume with vehicle trajectories is presented in Figures 6(a)–7(f). The trajectories of the vehicles are the expected trajectories of the gliders, projected to the ocean surface. Note that in Figures 6(a)–7(f), we only display a trajectory for a vehicle at the hour when it surfaces due to the offset in start times. The predicted extent of the plume is delineated by the closed polygon. The centroid of the predicted plume is depicted by the dot inside the delineated plume extent; the centroid-tracking vehicle follows the path given by the solid line and the boundary-tracking vehicles follow the paths given by the dashed lines.

The trajectory design is based upon model predictions, and we are familiar with the deployment area; we do have an *a priori* understanding of the general direction the feature should travel in. This knowledge can be used to select the initial locations of the vehicles based upon the information to be gathered and areas of interest within the feature. In this
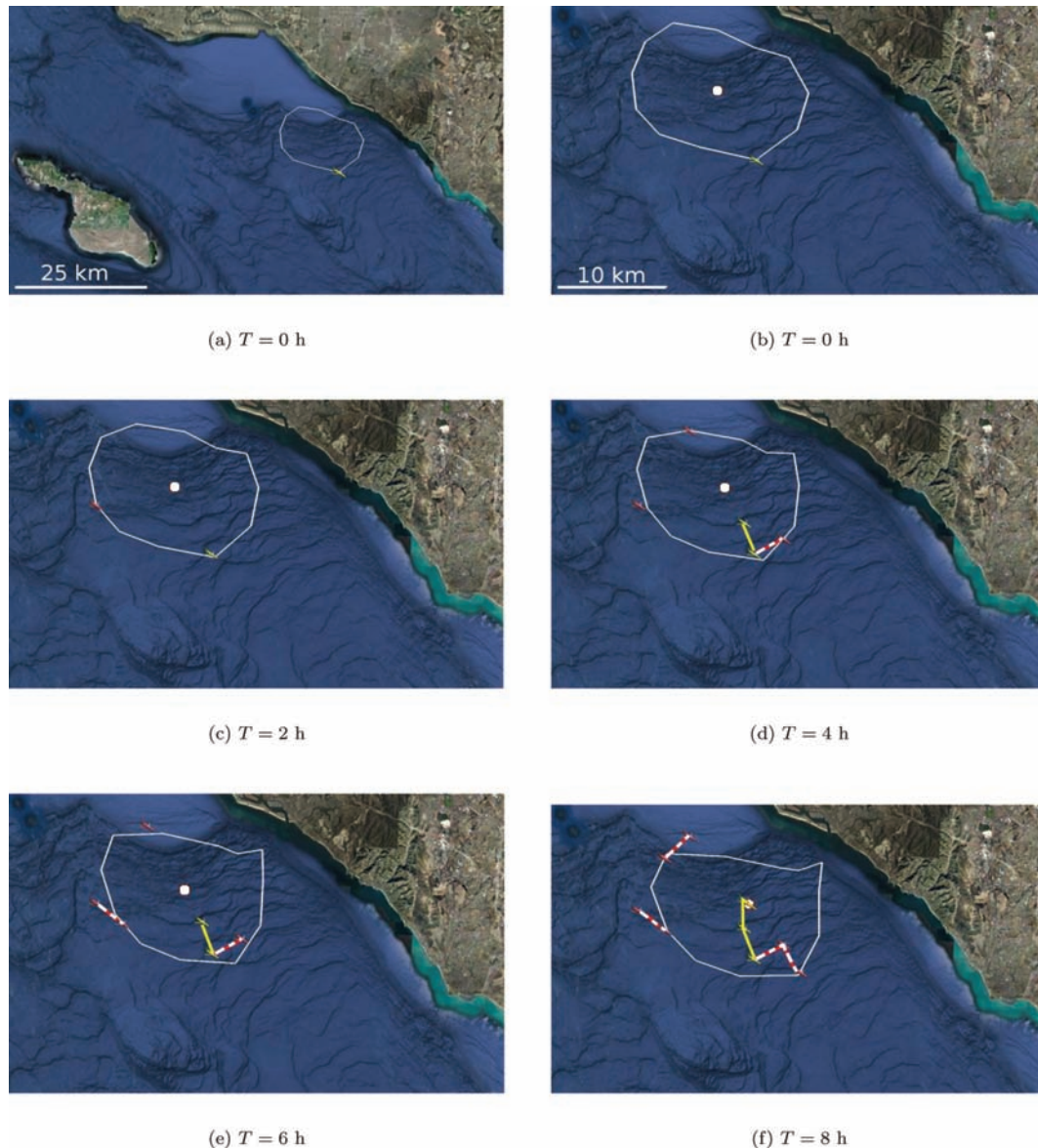
Fig. 6. Simulation results for four vehicles tracking a propagating plume. The plume extent is delineated by the closed polygon. Three vehicles (dashed line paths) follow the boundary, while one vehicle (solid line path) tracks the centroid of the plume. The centroid is depicted by the dot inside the delineated plume extent. Panel (a) provides the initial delineation of the plume in the coastal region near Los Angeles, CA. Panel (b) presents an enlarged image of panel (a). Panels (b)–(f) present snapshots every 2 h of the tracking simulation from initialization to $T = 8$ h. The scale given in panel (b) is the same for panels (c)–(f). Images created by use of Google Earth.

example, since we see a rather fast-moving feature in the southeast direction, we choose to start the centroid tracker on the southern extent, or leading edge, of the feature. Thus, we do not try and *chase* the area we are interested in sampling, and have a higher probability of collecting data within the plume. Based on the movement of the feature, the centroid-tracking vehicle (solid line) actually completes a U-shape trajectory, and from $T = 12$ to 16h cannot keep up with the feature, based on our constant-speed assumption. We also see the speed of the feature since

the boundary-tracking vehicles (dashed lines) traverse more of a straight-line path than the zig-zag seen with a slower-moving feature as in Figures 11(f) and 12(e). Overall, the trajectories presented here, and in the previous deployment sections, do not resemble those that a human operator would design. However, the trajectories do guide the vehicles through a large portion of the plume during its predicted evolution, thus increasing the probability of collecting high-valued data for both the marine biology community and the modeling community alike.
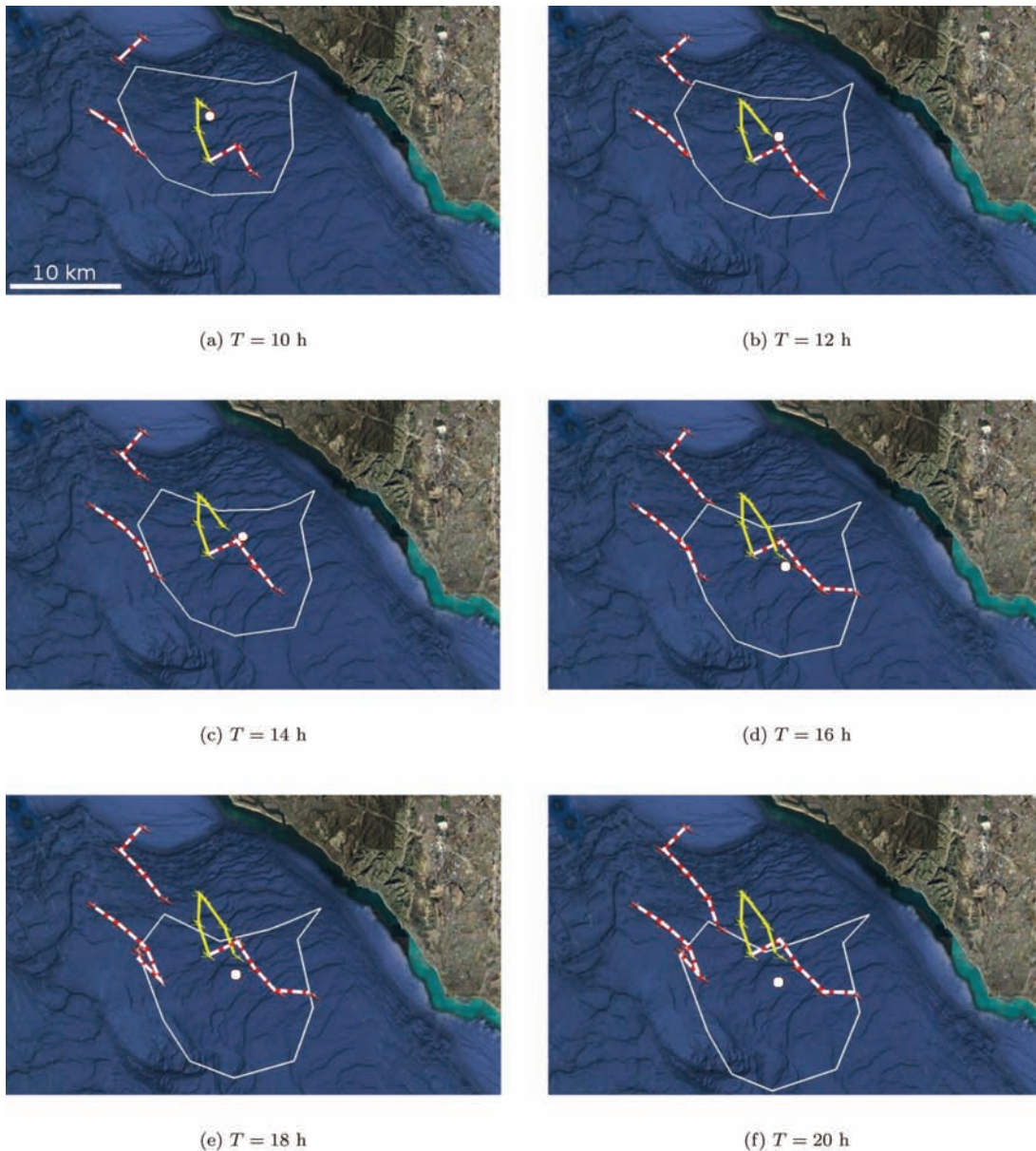
Fig. 7. Continuation of the simulation results for four vehicles tracking a propagating plume presented in Figure 6. The plume extent is delineated by the closed polygon. Three vehicles (dashed line paths) follow the boundary, while one vehicle (solid line path) tracks the centroid of the plume. The centroid is depicted by the dot inside the delineated plume extent. Panels (a)–(f) present snapshots every two hours of the tracking simulation from $T = 10$ h to completion ($T = 20$ h). The scale for all images is given in panel (a). Images created by use of Google Earth.

7. Implementation and Field Experiments in the SCB

We present the results of two field deployments, during which we implemented trajectories designed by Algorithm 3. In Section 7.1 we present the results of a single-vehicle, centroid-tracking mission initially presented in Smith et al. (2009a). We follow this in Section 7.2 with a two-vehicle mission, tracking both the centroid and the boundary of a plume. We remark to the reader that the

implementation of the path plans generated here would ideally be implemented and executed in an opportunistic fashion onto a currently deployed vehicle. In this case, the ability to select the initial location of the vehicle with respect to the feature of interest is not practical. In the following field trials, the vehicles were on a routine deployment and the presented experiments are meant to simulate an opportunistic retasking event. Note that the plume we wish to track is delineated close to near-future

surfacing locations of the gliders so that missions can be uploaded and executed in a timely fashion, and the vehicles can continue with the previous routine survey. Initial locations of the vehicles with respect to the plume delineation are purposefully chosen to be suboptimal to present a real-life situation. An alternate scenario to opportunistic retasking is to consider that the vehicles are deployed specifically for a detected algal bloom or river plume. This situation has been addressed in the simulation experiment presented in Section 6.

As noted in Smith et al. (2009a), the rainy season in Southern California is generally between November and March. During this time, storm events cause large runoff into local-area rivers and streams, all of which empty into the Pacific Ocean. Two major rivers in the Los Angeles area, the Santa Ana and the Los Angeles River, input large freshwater plumes to the SCB. Such plumes have a high likelihood of producing HABs. Unfortunately, during both deployments, weather and/or remote-sensing devices did not cooperate to produce a rain event along with a detectable plume. For both cases presented here, we defined a pseudo-plume in two separate areas of the SCB to demonstrate a proof-of-concept of the technology chain and trajectory design method developed here.

For the centroid-tracking mission, we deployed a glider into the SCB on 17 February 2009 to conduct a month-long observation and sampling mission. For this deployment, the glider was programmed to execute a zig-zag pattern mission along the coastline, as depicted in Figure 8, by navigating to each of the six waypoints depicted by the bullseyes. During execution of this mission, we retasked the glider mid-mission and uploaded the centroid-tracking trajectory described in Section 7.1.

For the boundary-tracking mission, we deployed two gliders off the northeast tip of Santa Catalina Island on 29 April 2009 to conduct a month-long experiment to test the communication infrastructure described in Smith et al. (2010a). For this mission, there was not a single, predetermined path for the glider to traverse as before, but we had the ability to retask the vehicles as needed. The details of this mission, with regard to the communication data collected, can be found in Pereira et al. (2009) and Smith et al. (2009b). The 2-day mission presented below was conducted during 11–13 May 2009.

7.1. Centroid Tracking

The mission presented in this section is reproduced from Smith et al. (2009a). Since Algorithm 1 has been modified based on the lessons learned during the execution of this deployment, there are slight discrepancies in planning between the following description and the method presented in Algorithm 1. However, the general idea and methodology is the same.

For this mission, we defined a pseudo-plume $\mathcal{D}$ with 15 initial drifter locations off the coast of Newport Beach, CA. The pseudo-plume is given by the dashed line in Figure 9.
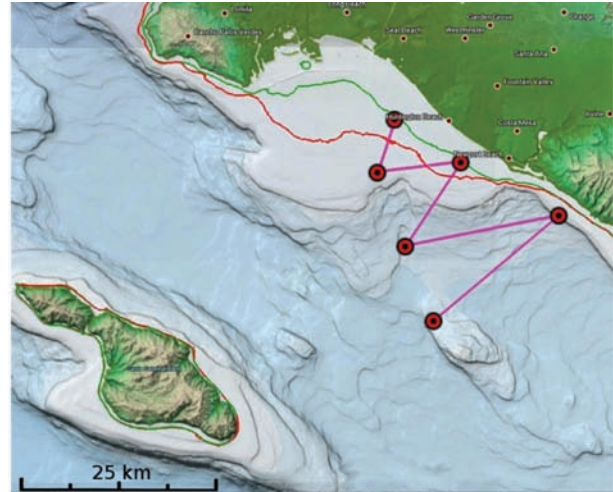

Fig. 8. The intended glider path of the month-long, zig-zag pattern mission started on 17 February 2009 is given by the solid line. The preset waypoints that define this path and were uploaded to the glider are depicted by the bullseyes. This path represents a routine deployment mission carried out regularly by USC CINAPS gliders. Image created by use of Google Earth.
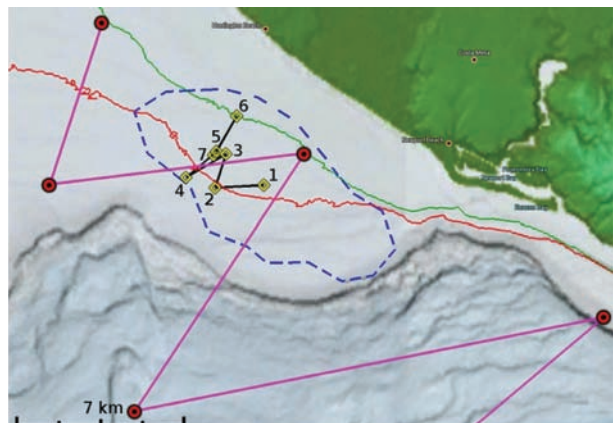

Fig. 9. An overview of the delineated plume to track and the computed path to track the centroid of the plume. The solid line connecting bullseyes represents the routine zig-zag mission presented in Figure 8. The initial delineation of the plume to track is given by the dashed line. The waypoints generated by Algorithm 1 are represented by the numbered diamonds. The intended glider path (projected to the ocean surface) is the solid line connecting the consecutively numbered waypoints. Image created by use of Google Earth.

By use of ROMS, the locations of the points in $\mathcal{D}$ were predicted for $T = 15$ h. The initial time and location for the beginning of this retasking experiment coincided with predicted coordinates of a future glider communication. The pseudo-plume was chosen such that C_0 was near this predicted glider surfacing location.

Based on observed behavior for our vehicle during this deployment, we take $v = 0.75$ km h^{-1}, and initially defined

Table 1. A Complete Listing of the Waypoints Generated by Algorithm 1. Waypoint Numbers 1, 3, 5 and 7 are the Predicted Centroids of the Pseudo-plume at Hours 0, 5, 10 and 15, Respectively. Waypoint Numbers 2, 4 and 6 are the Additional Locations ($p^* \in \mathcal{L}$) to be Visited as Computed in Case 2 ($d_g(L, C_4) \leq d_l$) of Algorithm 1

Number	Latitude (° N)	Longitude (° E)	Number	Latitude (° N)	Longitude (° E)
1	33.6062	−118.0137	5	33.6189	−118.0349
2	33.6054	−118.0356	6	33.6321	−118.0257
3	33.6180	−118.0306	7	33.6175	−118.0361
4	33.6092	−118.0487			

$d_l = 0.5$ km and $d_u = 0.8$ km. The hourly predictions were input to the trajectory design algorithm and a tracking strategy was generated. Due to slow projected surface currents in the area of study, the relative movement of the plume was quite small. To keep the glider from surfacing too often and to generate a more implementable trajectory, we opted to omit visiting consecutive centroids. Instead, we chose to begin at the initial centroid, then visit the predicted centroid of the plume after 5, 10 and 15 h, C_5, C_{10} and C_{15}, respectively. Between visiting these sites, the algorithm computed an additional waypoint for the glider to visit. These intermediate waypoints were chosen similarly to the p^* defined earlier, with $d = 3.75$ km; the distance the glider should travel in five hours. This design strategy produced seven waypoints for the AUV to visit during the 15 h mission. The waypoints are presented in Table 1. Note that we include the initial centroid as a waypoint, since the glider may not surface exactly at the predicted location.

Upon visiting all of the waypoints in Table 1, the glider was instructed to continue the sampling mission shown in Figure 8. Figure 9 presents a broad overview of the waypoints in Table 1, along with a path connecting consecutive waypoints. The plume is delineated by the dashed line and the waypoints are numbered and depicted by numbered diamonds. Note that the glider did not travel on the ocean surface during this experiment. As previously mentioned, between waypoints the glider submerges and performs consecutive dives and ascents creating a sawtooth-shaped trajectory as its glide path.

7.1.1. Analysis of Results Next, we present the implementation results of the aforementioned sampling mission onto a glider operating in the SCB. The waypoints given in Table 1 were computed under the assumption that the mission would be loaded onto the glider at a specific time and approximate geographical location. The glider arrived and communicated at the correct time and location; however, communication was aborted before the plume tracking mission could be uploaded. We were able to establish a connection two hours later at a different location, and successfully upload the mission file; this location is the droplet labeled 1 in Figure 10. We opted to not visit waypoint 1 based on the location of the glider and to get the glider back on schedule to track the plume. Figure 10 presents a magnified image of Figure 9, where computed

Fig. 10. Execution of the computed path for tracking the centroid of an evolving plume. The initial delineation of the plume to track is given by the dashed line. The waypoints generated by Algorithm 1 are represented by the numbered diamonds. The actual locations where the glider surfaced are given by the numbered droplets. The intended path of the glider (projected to the ocean surface) is the solid line path connecting the numbered diamonds. Image created by use of Google Earth.

waypoints are the numbered diamonds and the numbered droplets are the actual locations visited by the glider.

We were able to successfully generate a plan and retask a deployed glider to follow an ocean feature for 15 h. It is clear from the data that consideration has to be made for glider dynamics and external forcing from ocean currents in the path planning process. This is an area of ongoing research; see Smith et al. (2010b,c).

One element that we have neglected to discuss up to this point is that we have no metric for comparison. In particular, when we reach a predicted centroid, we do not have a method to check whether or not the plume centroid was actually at that location. We are planning experiments to deploy actual Lagrangian drifters to simulate a plume, as well as hoping for an actual event to present itself. This will give a concrete comparison between the ROMS prediction and the actual movement of the drifters or the plume. Another component omitted from earlier discussion is time. When tracking a moving feature, a predicted waypoint contains temporal information as well as location. For this implementation, the glider began the mission at 0302Z and

Table 2. A Complete Listing of the Waypoints Generated by Algorithm 1 for Both Days of the Multi-vehicle Plume Tracking Mission Presented in Section 7.2. The Left-hand Columns give the Selected Waypoints for Day One and the Right-hand Columns give the Waypoints for Day Two of the Mission. These Waypoints Define the Implemented Paths for the Centroid-tracking Vehicle. For the First Day, Waypoint Numbers 1, 2, 3, 4 and 6 are the Computed Surfacings for the Glider at Hours 0, 4, 8, 12 and 16, Respectively. Waypoint Number 5 is an Additional Location ($p^* \in \mathcal{L}$) to be Visited as Computed in Case 2 ($d_g(L, C_4) \leq d_l$) of Algorithm 1. For the Second Day, Waypoint Numbers 1, 3, 5, 6 and 7 are the Computed Surfacings for the Glider at Hours 0, 4, 8, 12 and 16, Respectively. Waypoint Numbers 2 and 4 are Additional Locations ($p^* \in \mathcal{L}$) to be Visited as Computed in Case 2 ($d_g(L, C_4) \leq d_l$) of Algorithm 1

Day 1	Latitude (° N)	Longitude (° E)	Day 2	Latitude (° N)	Longitude (° E)
1	33.5180	−118.3930	1	33.5060	−118.4970
2	33.5281	−118.4230	2	33.5236	−118.4810
3	33.5266	−118.4553	3	33.5241	−118.4901
4	33.5177	−118.4859	4	33.5060	−118.4781
5	33.5232	−118.4826	5	33.5118	−118.4809
6	33.5061	−118.4968	6	33.4867	−118.4688
			7	33.4608	−118.4523

Table 3. A Complete Listing of the Waypoints Generated by Algorithm 2 for Both Days of the Multi-vehicle Plume Tracking Mission Presented in Section 7.2. The Left-hand Columns give the Selected Waypoints for Day One and the Right-hand Columns give the Waypoints for Day Two of the Mission. These Waypoints define the Implemented Paths for the Boundary-tracking vehicle

Day 1	Latitude (° N)	Longitude (° E)	Day 2	Latitude (° N)	Longitude (° E)
1	33.5350	−118.5600	1	33.5350	−118.5600
2	33.5612	−118.5526	2	33.5081	−118.5584
3	33.5759	−118.5254	3	33.5332	−118.5466
4	33.5530	−118.5424	4	33.5201	−118.5183
5	33.5693	−118.5167	5	33.4974	−118.5357

ended at 1835Z; a total time of 15.55 h. Owing to external disturbances, arrival at a few waypoints was not at the predicted times. The primary external disturbance affecting temporal, and spatial, accuracy is ocean currents. As previously mentioned, extensions to Algorithm 3 have been made in Smith et al. (2010c) to design more temporally feasible paths for the glider while tracking the centroid of a plume.

7.2. Centroid and Boundary Tracking

For this mission, we defined a pseudo-plume $\mathcal{D}$ with 12 initial drifter locations off the northeast coast of Santa Catalina Island. Again, based on observed behavior, we take $v = 0.75$ km h^{-1}, and define $d_l = 2.7$ km and $d_u = 3.3$ km. An overview of the general testing area for this deployment is presented in Figure 11(a). By use of ROMS, the locations of the points in $\mathcal{D}$ were predicted for $T = 16$ h. Owing to the predicted currents and proximity to Catalina Island, two of the initially defined drifters exited the model boundary. Thus, the plume was propagated and computations were made by use of 10 drifters.

7.2.1. Analysis of Results This retasking mission further validated the proof-of-concept of generating and implementing trajectories by use of predictive ocean models.

In this case, we demonstrated further functionality by incorporating multiple vehicles and testing the iterative capabilities of the proposed technique by closing the loop with data assimilation into ROMS to update the next prediction. Since we used a pseudo-plume as a tracking proxy, we again do not have a metric in this experiment to assess any change in skill of ROMS predictions due to the data assimilation conducted. However, it is worth noting that collected data were successfully transmitted and assimilated from the robot in the field to ROMS for use in the next prediction. Using the methods described here to generate trajectories for multiple vehicles is not difficult. The complexity arises in synchronizing surfacings or compensating for asynchronous communication with the fleet of gliders. This synchronization problem was addressed in Paley et al. (2008) for their specific application, and it is of interest to us to implement a similar, high-level control system to aid in the facilitation and management of multi-vehicle deployments incorporating autonomous retasking. Preliminary infrastructure and research towards this goal is presented in Smith et al. (2010a) and Pereira et al. (2009).

To begin, the plume was delineated in an area of current operation of two deployed gliders. The initial location is presented in Figure 11(b). The waypoints computed by Algorithm 3 to follow this plume are presented for the
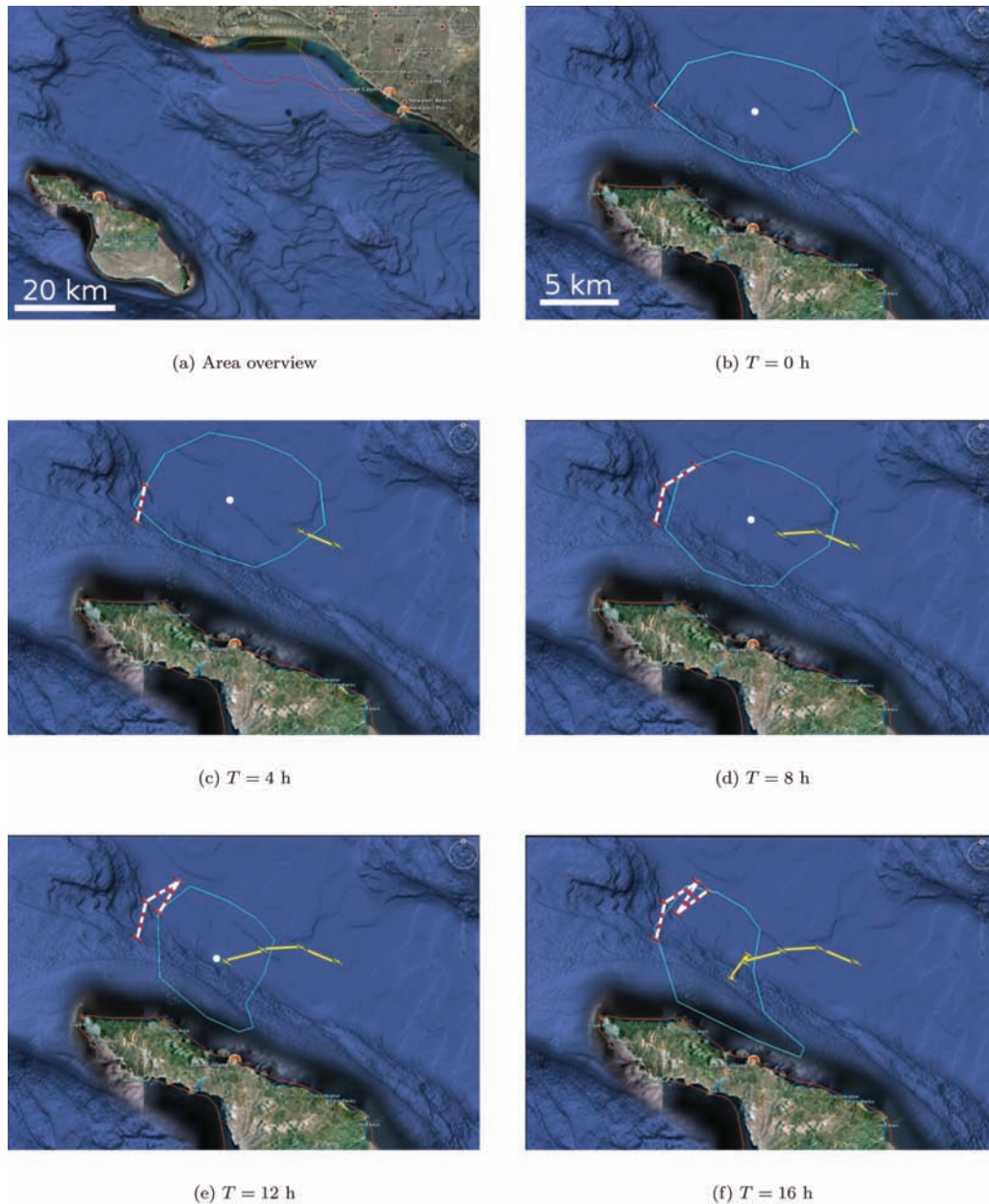
Fig. 11. Deployment results for the first day of the mission for two vehicles to track an evolving plume. The plume extent is delineated by the closed polygon. One vehicle (dashed line path) follows the boundary, while one vehicle (solid line path) tracks the centroid of the plume. The centroid is depicted by the dot inside the delineated plume extent. Panel (a) provides an overview of the deployment area off the coast of Los Angeles, CA. Panel (b) presents an enlarged image of the deployment area just off the northeast coast of Santa Catalina Island, CA with the initial delineation of the plume. Panels (b)–(f) present snapshots every four hours of the tracking experiment from initialization to completion (*T* = 16 h) for the first day. The scale given in panel (b) is the same for panels (c)–(f). Images created by use of Google Earth.

centroid- and boundary-tracking vehicles in the left-hand columns of Tables 2 and 3, respectively. The initial time and location for the beginning of this retasking experiment coincided with predicted coordinates of glider surfacings. Since the assigned mission was to collect communication data, the vehicles were surfacing frequently (∼ 2 h intervals). This made coordinating surfacing time much more manageable than in the scenario presented in Section 7.1, where the glider was surfacing approximately every 8 h. In addition, communication via our implemented Freewave™ network (Pereira et al. 2009) facilitated more robust communication, as well as more rapid file exchange than during previous deployments. Once both gliders were on the surface together (approximately 1800Z, 11 May

2009), we ran Algorithm 3 with the location of each glider initially being on the boundary of the plume. Figure 11(b)(f) display the delineation of the plume with the locations of both gliders at 4-h increments from $T = 0$ h (Figure 11(b)) to $T = 16$ h (Figure 11(f)). In these figures, the boundary-tracking glider follows the dashed line and the centroid-tracking glider follows the solid line. The respective icons along the paths denote the locations where the glider surfaced while executing the mission. When visible, the dot inside the polygonal delineation of the plume extent represents the predicted centroid of the plume; when not seen, the centroid-tracking glider surfaced within 500 m of the location of the predicted centroid. The solid and dashed lines depict the path of the glider (projected to the surface) between surfacings. Note that in the initial four hours of the mission, the plume moved northward, and the boundary-tracking vehicle was on the leading edge. However, after the initial few hours, the plume migrated southward and the boundary-tracking glider ended up following the trailing edge of the plume. Day one of this mission ended shortly after 1000Z on 12 May 2009.

Upon completion of the day-one mission, the gliders resumed their previous missions of gathering communication data while we awaited the following day's ROMS prediction. The entire process mentioned above was repeated beginning at approximately 2200Z on 12 May 2009. The initial plume delineation, glider surfacing locations and projected trajectories are given in Figure 12(a-e). The computed waypoints for the centroid- and boundary-tracking vehicles are given in the right-hand columns of Tables 2 and 3, respectively. Day two of the mission completed shortly after 1400Z on 13 May 2009. Note that at the start of day two, we redelineated the plume differently from the final predicted configuration of day one. This is applicable in practice because we cannot assume ROMS to be 100% accurate, and we have a time gap between the start of the sampling missions where we expect the plume to further evolve. Additionally, we are forecasting the evolution of a plume based on the predicted paths of multiple, unconnected, Lagrangian drifters, which may not behave exactly like a contiguous ocean feature.

Overall, this 2-day mission validated both the multi-vehicle applicability as well as the ability to close the loop on the technology toolchain from ROMS to path planning to field AUV and back to ROMS. This further motivates our efforts to prepare for a large-scale deployment, such as Bight 2010 presented in Section 6, with hopes of locating and tracking a plume from a significant rain event runoff, or a HAB.

8. Conclusions and Future Work

In the study of path planning for field robots, designing the trajectory is usually less than half the battle; the real challenge comes in the implementation. This is exaggerated when dealing with underwater robots due to the complex,

and often unknown, environment. Poorly understood ocean dynamics, difficulty in localization and extreme conditions all contribute to the struggle of successful implementation of a planned mission for an AUV. In this paper, we examined the use of ocean model predictions to help reduce some of this uncertainty for the application of path planning to track an evolving ocean feature.

Generating effective sampling strategies to study ocean phenomena is a challenging task that can be approached from many different angles. Here we presented a method to exploit multiple facets of technology to achieve our goal. Utilizing an ocean model, an embedded sensor network and an AUV, we were able to construct a technology chain which plans a path to track areas of scientific interest within a chosen feature of interest for a chosen period of time. This toolchain was used to design a single-vehicle mission to track a plume's centroid, and generate the paths for a multi-vehicle mission for simultaneous sampling at the centroid as well as along the boundary of a given feature. We presented iterated field trials to demonstrate closing the loop of the technology chain developed as well as to demonstrate a proof-of-concept of the planning method presented. This paper has demonstrated that we have implemented the collaboration and technology chain required to perform complex field experiments to track dynamically evolving ocean features. Research is ongoing to extend and improve upon the presented waypoint-generation and path planning algorithms to incorporate ROMS 4-D velocity predictions to improve the accuracy of the implementation (Smith et al. 2010c). Additionally, we are interested in assessing the accuracy of ROMS velocity predictions, and the performance and reliability of our gliders to more effectively utilize them to further our understanding of the life cycle of an algal bloom (Smith et al. 2010b). We remark that the implementation and realization of the paths generated in this paper were perfectly feasible, given that there was no temporal constraint. Improving the temporal feasibility along with the spatial accuracy is a primary focus of ongoing and future work in this area. Based on the operational constraints of the gliders, these are not the optimal vehicles to chase fast-moving events or adaptively react to dynamically changing conditions. The CINAPS team is in the process of acquiring a different type of AUV that is more agile and can more effectively carry out the strategies designed here, with specific regard to fast-moving features.

The main implementation issue is the assumed ability of the glider to accurately navigate to a given waypoint. In general, this is a widely studied, and currently unsolved, problem in underwater robotics. For the results presented here, this artifact is a result of the waypoint-selection algorithms only utilizing a 2-D propagation of the plume, and ignoring the dynamics of the glider and predicted vertical velocity profiles when generating the final path plan. Research is active to extend these results to incorporate the kinematic and dynamic aspects of the
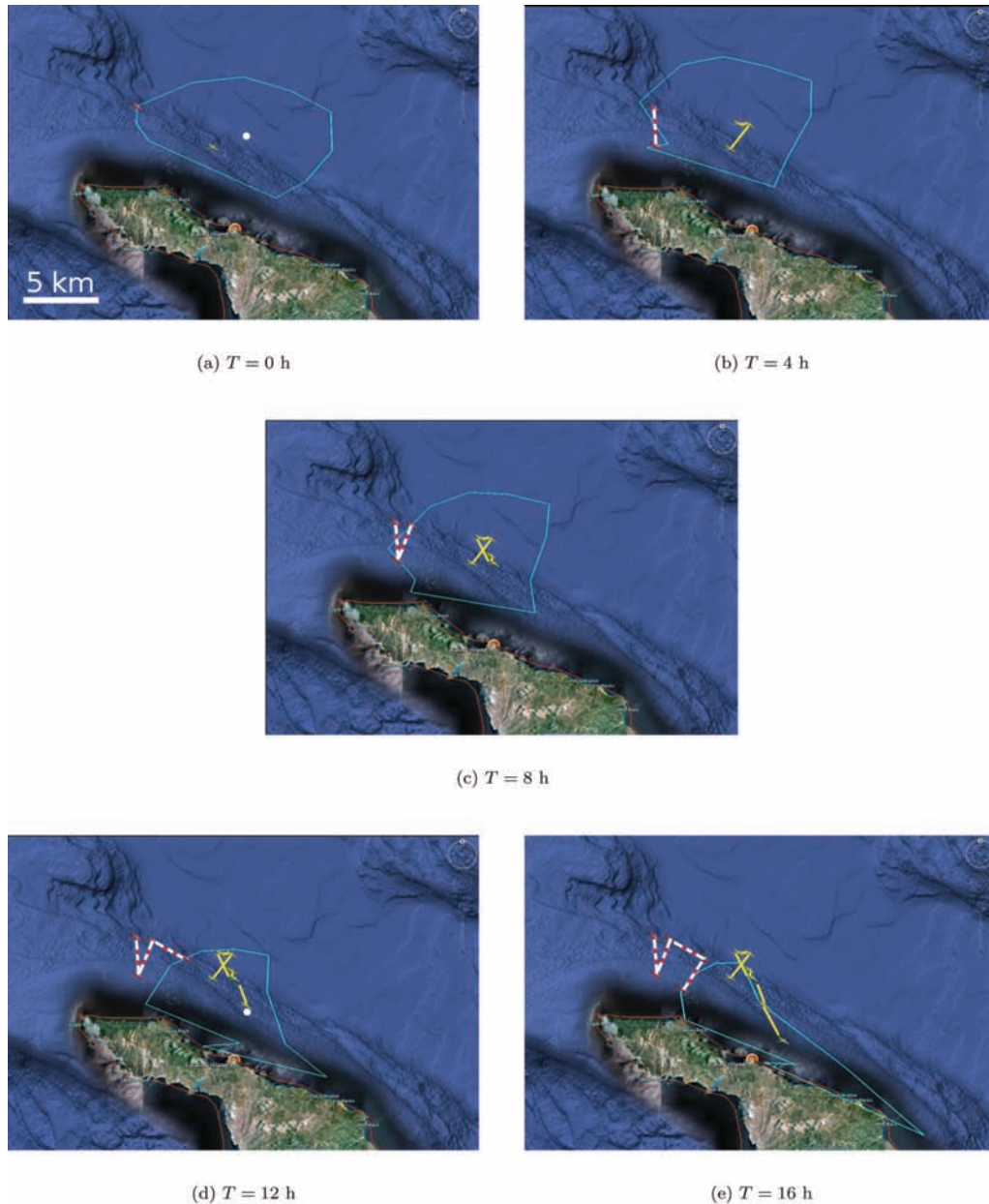
Fig. 12. Deployment results for the second day of the mission for two vehicles to track an evolving plume. The plume extent is delineated by the closed polygon. One vehicle (dashed line path) follows the boundary, while one vehicle (solid line path) tracks the centroid of the plume. The centroid is depicted by the dot inside the delineated plume extent. Panel (a) presents an enlarged image of the deployment area just off the northeast coast of Santa Catalina Island, CA with an updated delineation of the plume for the start of day two. Panels (a)–(e) present snapshots every four hours of the tracking experiment from initialization to completion ($T = 16$ h) for the second day. The scale given in panel (a) is the same for panels (b)–(e). Images created by use of Google Earth.

glider, see Smith et al. (2010b), and extend this method of path planning from a planar to a 3-D path planning algorithm and trajectory generation toolchain, see Smith et al. (2010c). As mentioned previously, we are making progress to increase the performance of the AUV through the use of ocean model predictions, but at this time we are still not equipped to utilize ROMS predictions to propagate a feature of interest in 4-D. The primary reason

for this is based on the lack of understanding and detection capabilities of the initial 3-D structure and extent of a given plume. Algal blooms, in particular, are too poorly understood to hypothesize about their 3-D spatial extent; we currently have difficulties determining and predicting their 2-D extent.

A long-term goal of this effort is to utilize the embedded sensor network presented in Smith et al. (2010a) and

Pereira et al. (2009) to enable real-time, optimal trajectory design, based on ocean model predictions, to gather *in situ* measurements of interesting and evolving ocean features and phenomena while additionally increasing the skill of regional ocean models. Through this effort, we aim to quantitatively assess the effectiveness of ocean model predictions in the design and accurate implementation of trajectories for AUVs. As previously mentioned, this will come with deployment of actual drifters simulating the propagation of a feature, or the occurrence of an actual HAB event during Bight 2010.

As discussed in Section 6, a more immediate implementation of the methods developed here will be used during our participation in Bight 2010. Currently, we are experiencing weak El Niño conditions, as equatorial Pacific, sea-surface temperatures remained above average through August 2009. These conditions are expected to strengthen through winter 2009–2010 in the Northern Hemisphere (Climate Prediction Center 2009), and have impacted Southern California with more frequent and intense storm events in early 2010. From the discussion in Sections 2.1 and 2.2, we can infer that the potential for the formation of conditions that may promote an algal bloom is increased over the next year. Such information presents a greater opportunity to retest and validate our methods and algorithms in a real scenario. Thus, we are motivated to further develop our algorithms to steer AUVs into locations of high scientific merit with regard to HAB research and help ocean scientists better understand these complex phenomena, while additionally assessing the prediction capabilities of regional ocean models.

Acknowledgements

Notes

1. The SCB is the oceanic region contained within 32° N to 34.5° N and −117° E to −121° E.
2. The SCB is a very high traffic region, and the glider has a low visual profile when on the surface. Although the probability of a collision is low, we choose to err on the side of caution.

References

Anderson, D. (2008). Harmful algae, http://www.whoi.edu/redtide/page.do?pid=9257 (accessed February 2009).

Cetinic, I., Jones, B. H., Moline, M. A. and Schofield, O. (2010). Resolving urban plumes using autonomous gliders in the coastal ocean, *Continental Shelf Research*.

Chao, Y., Li, Z., Farrara, J., McWilliams, J. C., Bellingham, J., Capet, X., et al. (2008). Development, implementation and evaluation of a data-assimilative ocean forecasting system off the central California coast, *Deep-Sea Research II*, 56: 100–126.

Climate Prediction Center (2009). El Niño/Southern Oscillation (ENSO) diagnostic discussion, http://www.cpc.noaa.gov/products/analysis_monitoring/enso_advisory/ensodisc.html (accessed September 2009).

Dailey, M. D., Reish, D. J. and Anderson, J. W. (eds.) (1993). *Ecology of the Southern California Bight*. Berkeley, CA, University of California Press.

Das, J., Rajan, K., Frolov, S., Ryan, J., Py, F., Caron, D. A. and Sukhatme, G. S. (2010). Towards marine bloom trajectory prediction for AUV mission planning. *IEEE International Conference on Robotics and Automation*, http://cres.usc.edu/cgi-bin/print_pub_details.pl?pubid=637.

Davis, R. E., Ohman, M., Rudnick, D., Sherman, J. and Hodges, B. (2008). Glider surveillance of physics and biology in the Southern California current system. *Limnology Oceanography*, 53: 2151–2168.

Fiorelli, E., Leonard, N., Bhatta, P., Paley, D., Bachmayer, R. and Fratantoni, D. (2006). Multi-AUV control and adaptive sampling in Monterey Bay, *IEEE Journal of Oceanic Engineering*, 31(4): 935–948.

Graver, J. G. (2005). *Underwater Gliders: Dynamics, Control and Design*. PhD Thesis, Princeton University.

Gray, A. M., Lee, C., D'Asaro, E. A., Perry, M. J., Fennel, K., Briggs, N., Rehm, E., Sackmann, B. S., Sieracki, M. E., Poulton, N. and Gudmundsson, K. (2008), The 2008 north atlantic spring bloom experiment: observations of a stationary eddy on the eastern flank of the Reykjanes Ridge. *American Geophysical Union, Fall Meeting 2008*, Abstract#OS31A-1252.

Jet Propulsion Laboratory (2009). JPL THREDDS Data Server catalog, http://ourocean.jpl.nasa.gov:8080/thredds/ catalog.html(accessed September 2009).

Kennedy, V. S., Twilley, R. R., Kleypas, J. A., Cowan, J. H. Jr and Hare, S. R. (2002). Coastal and marine ecosystems and global climate change. *Pew Center on Global Climate Change*.

Kudela, R. M., Ryan, J. P., Blakely, M. D., Lane, J. Q. and Peterson, T. D. (2008). Linking the physiology and ecology of cochlodinium to better understand harmful algal bloom events: a comparative approach, *Harmful Algae*,7(3): 278–292.

Leonard, N. and Graver, J. (2001). Model-based feedback control of autonomous underwater gliders, *IEEE Journal of Oceanic Engineering*, 26(4): 633–645.

Leonard, N. E., Paley, D., Lekien, F., Sepulchre, R., Fratantoni, D. M. and Davis, R. (2007). Collective motion, sensor networks and ocean sampling, *Proceedings of the IEEE*, 95(1), 48–74.

Li, Z., Chao, Y., McWilliams, J. and Ide, K. (2008a). A three-dimensional variational data assimilation scheme for the regional ocean modeling system: implementation and basic experiments, *Journal of Geophysical Research*, 113: C05002.

Li, Z., Chao, Y., McWilliams, J. and Ide, K. (2008b). A three-dimensional variational data assimilation scheme for the regional ocean modeling system, *Journal of Atmospheric and Oceanic Technology*, 25: 2074–2090.

Paley, D., Zhang, F. and Leonard, N. E. (2007). Control of coordinated patterns for ocean sampling, *International Journal of Control*, 80(7): 1186–1199.

Paley, D., Zhang, F. and Leonard, N. (2008). Cooperative control for ocean sampling: the glider coordinated control system, *IEEE Transactions on Control Systems Technology*, 16(4): 735–744.

Pereira, A., Heidarsson, H., Caron, D., Jones, B. and Sukhatme, G. (2009). An implementation of a communication framework for the cost-effective operation of slocum gliders in coastal regions. *Proceedings of the 7th International Conference on Field and Service Robotics*, Cambridge, MA.

Schnetzer, A., Miller, P. E., Schaffner, R. A., Stauffer, B., Jones, B. H., Weisberg, S. B., DiGiacomo, P. M., Berelson, W. M. and Caron, D. A. (2007). Blooms of pseudo-nitzschia and domoic acid in the San Pedro channels and Los Angeles harbor areas of the Southern California Bight, 2003–2004, *Harmful Algae*, 6(3): 372–387.

Schofield, O., Kohut, J., Aragon, D., Creed, E., Graver, J., Haldman, C., Kerfoot, J., Roarty, H., Jones, C., Webb, D. and Glenn, S. (2007). Slocum gliders: robust and ready, *Journal of Field Robotics*, 24(6): 473–485.

Shchepetkin, A. and McWilliams, J. (1998). Quasi-monotone advection schemes based on explicit locally adaptive dissipation, *Monthly Weather Review*, 126: 1541–1580.

Shchepetkin, A. F. and McWilliams, J. C. (2005). The regional oceanic modeling system (ROMS): a split-explicit, free-surface, topography-following-coordinate oceanic model, *Ocean Modeling*, 9: 347–404.

Smith, R. N., Chao, Y., Jones, B. H., Caron, D. A., Li, P. P. and Sukhatme, G. S. (2009a). Trajectory design for autonomous underwater vehicles based on ocean model predictions for feature tracking. *Proceedings of the 7th International Conference on Field and Service Robotics*, Cambridge, MA.

Smith, R. N., Das, J., Heidarsson, H., Pereira, A., Caron, D. A., Jones, B. H. and Sukhatme, G. S. (2009b). Implementation of an embedded sensor network for the coordination of slocum gliders for coastal monitoring and observation. *WUWNet '09: Proceedings of the Fourth ACM International Workshop on Underwater Networks*. Berkeley, CA, ACM Press, pp. 1–8.

Smith, R. N., Das, J., Heidarsson, H., Pereira, A., Cetinić, I., Darjany, L., et al (2010a). USC CINAPS builds bridges: observing and monitoring the Southern California Bight, *IEEE Robotics and Automation Magazine*, 17: 20–30.

Smith, R. N., Kelly, J., Chao, Y., Jones, B. H. and Sukhatme, G. S. (2010b). Towards improvement of autonomous glider navigation accuracy through the use of regional ocean models. *Proceedings of the 29th International Conference on Offshore Mechanics and Arctic Engineering (OMAE 2010)*, Shanghai, China, June 2010. pp. 1–10.

Smith, R. N., Pereira, A. A., Chao, Y., Li, P. P., Caron, D. A., Jones, B. H. and Sukhatme, G. S. (2010c). Autonomous underwater vehicle trajectory design coupled with predictive ocean models: a case study. *Proceedings of the IEEE International Conference on Robotics and Automation*, Anchorage, AK. May 2010. pp 4770–4777.

U.S. Commission on Ocean Policy (2004). *An Ocean Blueprint for the 21st Century*. Washington, DC, http://oceancommission.gov/.

Vu, Q. (2008). JPL OurOcean portal, http://ourocean.jpl.nasa.gov/ (accessed February 2009).

Warrick, J. A. and Fong, D. A. (2004). Dispersal scaling from the world's rivers, *Geophysical Research Letters*, 31(4): L04301.

Webb Research Corporation (2008). http://www.webbresearch.com/slocum.htm (accessed May 2008).

Wood, E., Schnetzer, A., Benitez-Nelson, C., Anderson, C., Berelson, W., Burns, J., et al. (2009). The toxin express: rapid downward transport of the neurotoxin domoic acid in coastal waters, *Nature Geoscience*, 2: 273–275.